University of Pavia
Department of Molecular Medicine

PhD course in Translational Medicine
XXXVI cycle

*PhD thesis on*

# *Effects of repeated High-Intensity Interval Training interventions on oxidative metabolism adaptations in human skeletal muscle*

Tutor:
Prof.ssa Maria Antonietta Pellegrino

Candidate:
Emanuela Crea

Academic year 2020-2023

*A mia mamma e a mio papà per avermi trasmesso il valore della libertà.*
*A mio fratello Andrea, esempio di vita.*
*A Dario e alla sua dolcezza.*
*A te che non ci sei, ma che più di chiunque altro saresti stata fiera di me.*

*A tutti coloro che hanno creduto in me, fin dall'inizio fino alla fine.*

*"Ricorda che l'umiltà*
*Apre tutte le porte*
*E che la conoscenza*
*Ti renderà più forte*

*Lo sai che l'onestà*
*Non è un concetto vecchio*
*Non vergognarti mai*
*Quando ti guardi nello specchio*
*Non invocare aiuto nelle notti di tempesta*
*E non ti sottomettere, tieni alta la testa*

*Non frenare l'allegria*
*Non tenerla tra le dita*
*Ricorda che l'ironia*
*Ti salverà la vita*
*Ti salverà..."*

***In Viaggio*** *Fiorella Mannoia*

## List of scientific papers

1. Colosio M, Brocca L, Gatti MF, Neri M, **Crea E,** Cadile F, Canepari M, Pellegrino MA, Polla B, Porcelli S, Bottinelli R. **Structural and functional impairments of skeletal muscle in patients with post-acute sequelae of SARS-CoV-2 infection.** J Appl Physiol (1985). **2023** Oct 1;135(4):902-917. doi: 10.1152/japplphysiol.00158.2023. Epub 2023 Sep 7. PMID: 37675472.

2. Pilotto AM, Adami A, Mazzolari R, Brocca L**, Crea E**, Zuccarelli L, Pellegrino MA, Bottinelli R, Grassi B, Rossiter HB, Porcelli S. Reply to the letter from Manferdelli et al.: **'Muscle $O_2$ diffusion capacity by NIRS: a new approach in the air'.** J Physiol. 2022 Dec;600(23):5165-5166. doi: 10.1113/JP283919. Epub 2022 Nov 19. PMID: 36335427.

3. Pilotto AM, Adami A, Mazzolari R, Brocca L**, Crea E**, Zuccarelli L, Pellegrino MA, Bottinelli R, Grassi B, Rossiter HB, Porcelli S. **Near-infrared spectroscopy estimation of combined skeletal muscle oxidative capacity and $O_2$ diffusion capacity in humans**. J Physiol. **2022** Sep;600(18):4153-4168. doi: 10.1113/JP283267. Epub 2022 Aug 23. PMID: 35930524; PMCID: PMC9481735.

4. Sirago G, Toniolo L, **Crea E**, Giacomello E. **A short-term treatment with resveratrol improves the inflammatory conditions of Middle-aged muscle skeletal muscles**. Int J Food Sci Nutr. 2022 Aug;73(5):630- 637. doi: 10.1080/09637486.2022.2027889. Epub **2022** Jan 18. PMID: 35042437.

5. Toniolo L, Formoso L, Torelli L, **Crea E**, Bergamo A, Sava G, Giacomello E. **Long-term resveratrol treatment improves the capillarization in the skeletal muscles of ageing C57BL/6J mice**. Int J Food Sci Nutr. 2021 Feb;72(1):37-44. doi: 10.1080/09637486.2020.1769569. Epub **2020** May 24. PMID: 32449407.

6. Giacomello E, **Crea E**, Torelli L, Bergamo A, Reggiani C, Sava G, Toniolo L. **Age Dependent Modification of the Metabolic Profile of the Tibialis Anterior Muscle Fibers in C57BL/6J Mice.** Int J Mol Sci. **2020** May 30;21(11):3923. doi: 10.3390/ijms21113923. PMID: 32486238; PMCID: PMC7312486.

# INDEX

## Abstract

Skeletal muscle is a highly plastic tissue. Exercise is a potent stimulus that can remodel skeletal muscle by activating signaling pathways that change its metabolism and contractile properties. Resistance training is an effective intervention strategy to improve strength and muscle hypertrophy. It has been shown that an initial exposure to a hypertrophic stimulus leads to faster and greater growth of skeletal muscle if repeated subsequently. The permanence of acquired myonuclei and conserved epigenetic modifications are parallel processes that appear to be involved in the phenomenon known as 'muscle memory'.

Endurance exercise is a powerful tool for modulating mitochondrial biogenesis. Its ability to enhance the expression of key mitochondrial factors depends on the exercise intensity. Acute high-intensity endurance exercise has been shown to promote epigenetic modifications and gene expression of mitochondrial biomarkers more efficiently when compared to low-intensity exercise. Therefore, high-intensity endurance exercise could, in principle, trigger muscle memory processes.

This thesis aimed to examine whether two aerobic training interventions, separated by a period of training interruption, result in differential adaptations in oxidative metabolism and mitochondrial function.

To achieve this goal twenty healthy young subjects (aged 25 ± 5 years) underwent two repeated high-intensity interval training (HIIT) interventions (training and retraining), separated by 12 weeks of detraining in which exercise was completely discontinued. The training intervention consisted of 8 weeks of combined high-intensity cycling and interval sprint exercise performed 3 days per week. Maximal aerobic capacity and peak power output were measured *in vivo*. Mitochondrial respiration was measured ex-vivo using high-resolution respirometry. Gene and protein expression, histological analyses, and genome-wide DNA methylation were determined in-vitro on *vastus lateralis* biopsies.

Repeated HIIT interventions resulted in an improvement in aerobic fitness as indicated by the significant enhancement of peak oxygen consumption ($\dot{V}O_{2peak}$) and peak power output ($W_{peak}$) both after training and retraining. The increase of functional indexes of endurance performance paralleled the improvement in muscle capillarization (*capillary density and CD31 endothelial marker*) indicating that vascular changes in peripheral muscle work in conjunction with central changes to contribute to the gain of endurance performance. Endurance performance and

capillarization adaptations were not found different between the two HIIT interventions. Interestingly, the increase in CD31 content was retained during detraining.

Although no functional adaptation of mitochondria to the interventions was observed, the analyzed mitochondrial markers showed adaptations to high-intensity interval training that differed depending on whether the stimulus had been previously encountered. Mitochondrial biogenesis markers (*CS and PGC1α* protein content) tended to increase after training and significantly increased after retraining.

The protein content of *OPA1, MFN2* and *MFN1* showed a significant increase, indicating a pro-fusion mitochondrial adaptation after both training and retraining. As for mitochondrial biogenesis markers, MFN1 showed a tendency to increase after training, which became significantly higher after retraining. The observed protein adaptation profile was not affected by a transition in fibre types. Furthermore, the cross-sectional area of individual muscle fibres remained constant throughout the interventions, speculating that myonuclei incorporation did not significantly contribute to the observed increase in protein content.

Molecular data indicate that adaptations to retraining appear to be modulated by the initial training, suggesting a potential muscle memory mechanism triggered by endurance exercise. Based on these observations, the potential presence of an epigenetically based memory mechanism was investigated.

Genome-wide DNA methylation analysis revealed two memory profiles characterized by a state of hypomethylation that is acquired during training and maintained during detraining (with slight differences between the two signatures) and retraining. Six genes were identified as epigenetic memory genes. These genes showed a cumulative increase in gene expression during training and retention during detraining and retraining, which mirrored their hypomethylation profile. Since the retention of transcript expression was also observed in genes involved in lactate transport (*SLC16A3*), biomarkers of lactate transport (*MCT1, MCT4, LDH*) were studied. Following retraining, the content of MCT1 protein increased compared to the baseline, indicating a memory profile at the protein expression level. These data provide evidence for an epigenetically based memory mechanism, elicited by high-intensity aerobic training.

## LIST OF ABBREVIATIONS

| | |
|---|---|
| CAPN1 | calpain 1 |
| CAPN2 | calpain 2 |
| CpG | cytosine-phospate-guanine-3’ dinucleotide pairing |
| CREB | cyclic AMP-responsive element binding |
| CS | citrate synthase |
| DMP | differentially methylated position |
| DMR | differentially methylated region |
| Drp1 | dynamin-related protein 1 |
| Fis1 | fission protein 1 |
| HDAC | histone deacetylase |
| HIIT | high-intensity interval training |
| IGF-1 | insulin like growth factor 1 |
| *PDK4* | Pyruvate Dehydrogenase Kinase 4 |
| *PPARδ* | Peroxisome proliferator-activated receptor delta |
| INPP5a | inositol polyphosphate-5-phosphatase A |
| LDH | lactate dehydrogenase |
| MCT1 | monocarboxylate Transporter 1 |
| MCT4 | monocarboxylate Transporter 4 |
| MEF2 | myocyte-specific enhancer factors 2 |
| MFN1 | mitofusin 1 |
| MFN2 | mitofusin 2 |
| mtDNA | mitochondrial DNA |
| OPA1 | optic atrophy 1 |
| PGC-1α | peroxisome proliferator receptor-γ co-activator-1α |
| SERCA1 | sarcoplasmic/endoplasmic reticulum calcium ATPase 1 |
| SERCA2 | sarcoplasmic/endoplasmic reticulum calcium ATPase 2 |
| SIRT | sirtuin |
| SLC16A3 | solute carrier family 16-member 3 |
| SOM | self-organizing map |

# INTRODUCTION

## *Muscle plasticity*

The contractile activity of skeletal muscle can be altered by various stimuli, such as electrical stimulation, denervation, endurance exercise, resistance training, microgravity, nutritional interventions, hypoxia, and thermal stress. Additionally, skeletal muscle tissue undergoes gradual changes with ageing. At the structural level, skeletal muscle plasticity involves changes in the cellular (mitochondria, myofibrils, etc.) and extracellular (capillaries, nerves, connective tissue) compartments (*Schiaffino and Reggiani, 1996; Booth and Thomason, 1991*). Transcriptional reprogramming of nuclei is recognised as an important event in the early stages of this process (*Wittwer et al., 2002; Carson et al., 2001*). The role of signalling in the sensation and transduction of stimuli to activate specific gene expression events is widely recognised (*Flück and Hoppeler, 2003*). The process of skeletal muscle plasticity involves two mechanisms: the qualitative mechanism and the quantitative mechanism.

*The qualitative mechanism* is based on the presence of skeletal muscle fibre types with different functional properties. In mammalian adult muscle, four different fibre types can be distinguished: slow type I fibres and fast types IIA, IIX, and IIB fibres. Each of these fibre types is distinguishable due to the presence of a specific myosin heavy chain (MHC) isoform, which determines their contractile properties.

Slow type I fibres, also known as slow-twitch fibres, express the MHC-1 isoform and are rich in mitochondria, which provide the ATP needed to endure long-lasting muscle contractions without showing signs of fatigue. They rely on an aerobic metabolism, which is supplied with oxygen from the muscle's vascular system and myoglobin, a hemoprotein able to bind oxygen. Type IIB fibres express MHC-2B and are capable of powerful muscle contractions that require high quantities of ATP. However, the few mitochondria present in these fibres cannot support this high energy demand. Therefore, these muscle contractions are fueled by anaerobic metabolism, which does not require oxygen. Finally, fast type IIA and IIX fibres express MHC-2A and MHC-2X isoforms, respectively. These fibres have metabolic and functional properties that are intermediate between those of type I and type IIB. MHC-2B is typically only expressed in the skeletal muscle of small mammals and is not normally expressed at the protein level in human limb muscle (Schiaffino and Reggiani, 2011)

The muscle's ability to alter its functional and metabolic properties is facilitated by the heterogeneity of its fibre types and the ability to modify the relative content of each fibre type.

*The quantitative mechanism* alters the size of fibres, causing muscles to increase or decrease in size. Skeletal muscle mass can change rapidly in response to various stimuli, such as mechanical loads, nutrients, neural activity, cytokines, growth factors, and hormones (*Bodine, 2006; Sandri, 2008*). Cell size is determined by a balance between the accumulation of new proteins and the degradation of existing ones. Therefore, the pathways controlling protein synthesis and degradation play a crucial role in determining cell size.

Muscles grow in response to resistance exercise or anabolic hormonal stimulation because new proteins and organelles accumulate in the cytosol, increasing cellular volume. This process is called hypertrophy. Conversely, catabolic conditions such as cancer, infections, diabetes, organ failure, or inactivity/disuse promote a net loss of proteins, organelles, and cytoplasm causing shrinkage of the cellular volume. This condition is named atrophy. Therefore, the size and function of muscle cells are defined by the balance between biogenesis/biosynthesis and removal/destruction processes. The regulation of these pathways is controlled by autologous and nonautologous signals. The latter signals come from distal organs or from the interstitial cells that surround myofibers, including muscle stem cells (satellite cells) (*Sartori et al. Nature Communication 2021*).

### *Exercise training adaptations*

Exercise and physical activity, in their various forms, impose specific stresses on muscles. Depending on the type of stress, muscles may adapt by increasing size, improving neuromuscular performance, or enhancing endurance capabilities. This adaptive response can be induced by extracellular and intracellular factors, such as mechanical stretching, fluctuations in blood flow or temperature, an altered ATP/ADP ratio, or various hormones and systemic factors, parallel to exercise. These signals activate or repress multiple signalling pathways, which in turn regulate the transcription and translation of specific genes. The effects of these adaptations are functional and are influenced by the volume, intensity, and frequency of training, as well as the half-life of proteins (*Coffey and Hawley, 2007*).

Phenotypic adaptation induced by training is a response to repeated stimulation of single exercise sessions. Following a single exercise session, there is a rapid but transient increase in the relative mRNA expression of a specific gene during recovery. Changes in mRNA expression from basal levels peak between 3-12 hours after exercise cessation, and typically return to basal levels within 24 hours, with a time course specific to each gene.

Repeated training leads to a gradual increase in protein response to repeated, pulsed increases in relative mRNA expression. Therefore, adaptation to training over a long period is due to the cumulative influence of each acute exercise session leading to a new functional threshold. Due to the longer half-lives of proteins compared to mRNA, changes in protein content are more readily observable than changes in transcript expression in response to chronic training, as opposed to acute exercise (Figure 1).

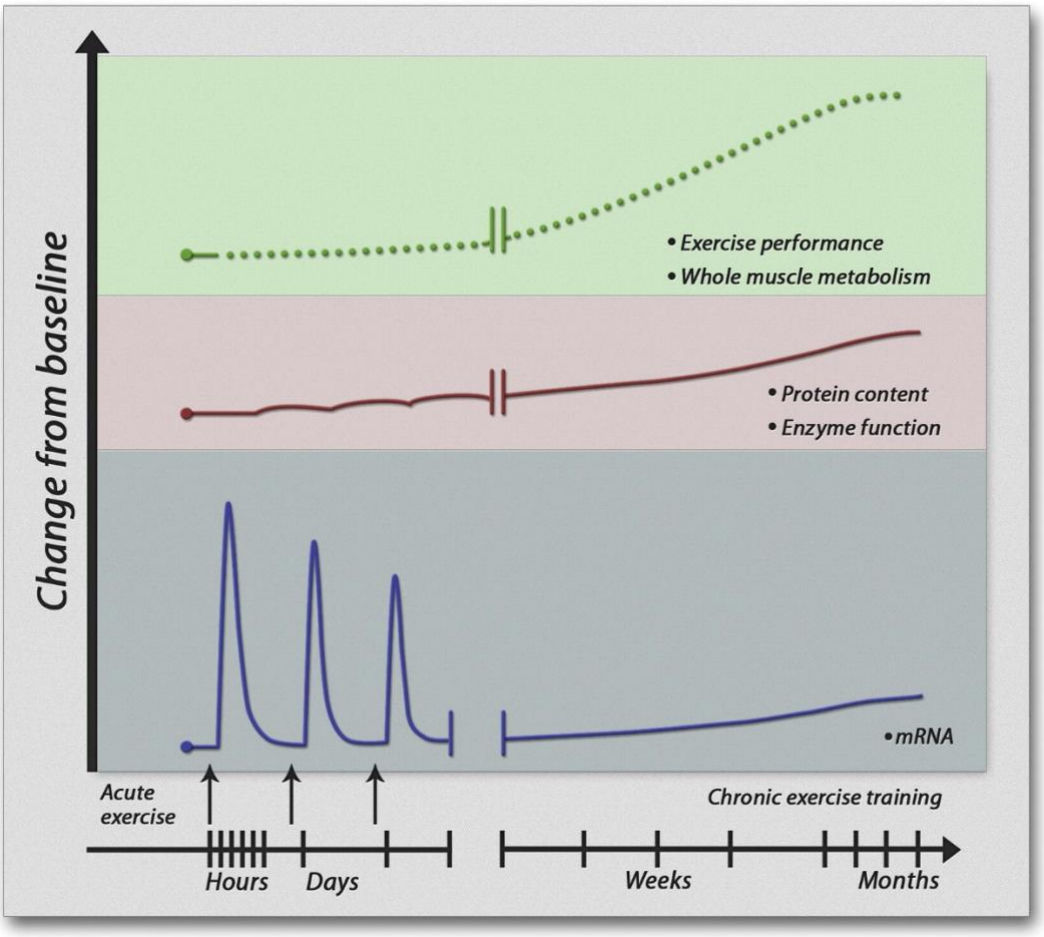


**Figure 1** Schematic representation of changes in mRNA expression (bottom panel) and protein content (middle panel) over time, as a consequence of acute and chronic (repetitive) exercise training.

Two main types of exercise training can be distinguished: strength or resistance training and endurance training. Resistance training involves higher loads at low

repetitions and focuses more on the work of the neuromuscular system. Traditional resistance exercise entails repetitions of dynamic concentric (muscle-shortening) and eccentric (muscle-lengthening) contractions against external load.

It is an effective intervention to increase skeletal muscle mass and strength (*Smith et al., 2023*). Endurance training, also known as aerobic exercise, on the other hand, involves low, repeated loads and focuses on the work of the cardiorespiratory system. It usually consists of continuous activity performed at low (<50% of $VO_{2max}$), moderate (~50-79% of $VO_{2max}$), or high intensities (≥80% of $VO_{2max}$) (*Smith et al., 2023).*

***Resistance training adaptations and muscle hypertrophy***

Resistance training leads to increases in muscle size, neural adaptations, and improved strength. These positive changes in physical capacity enable individuals to become stronger and more powerful (*Camera et al., 2016*).

At the molecular level, resistance exercise-induced skeletal muscle hypertrophy (defined as an increase in cross-sectional area (CSA) of singlemuscle fibres, and consequently of the whole muscle) occurs in adult humans because of the accrual of cellular proteins (e.g., myofibrillar, sarcoplasmic, mitochondrial) within pre-existing muscle fibres (Schoenfeld, 2010). Therefore, hypertrophy requires net muscle protein accretion, which occurs when the rate of muscle protein synthesis exceeds that of muscle protein breakdown. The effects of mechano-stimulation are molecularly transduced to downstream targets that shift muscle protein balance to favor synthesis over degradation.

*The signaling pathway IGF-1/PI3K/Akt* (growth factor like Insulin-1, phosphatidylinositol 3-kinase and protein kinase B, respectively) is considered the main mediator of normal muscle development and one of the most studied signaling molecular systems involved in muscle hypertrophy. This pathway plays a key role in the hypertrophic process, since it coordinates the molecular basis related to protein degradation and synthesis (*Sandri, 2008*). There are various stimuli that lead to the activation/phosphorylation of Akt, also known as protein kinase B (PKB): such as growth factors, cytokines, hormones, which occurs in a manner dependent on PI3K. PI3K phosphorylates phosphatidylinositol diphosphate (PIP2) and, thus, generates phosphatidylinositol triphosphate (PIP3), which in turn activates several effectors, including the kinase phosphoinositide-dependent kinase-1 (PDK1). PDK1 phosphorylates and activates Akt, which promotes the inactivation of tuberous

sclerosis complex 1/2 (TSC1/2) and the subsequent activation of mTOR. mTOR forms two different protein complexes, the rapamycin-sensitive mTORC1, when bound to Raptor, and the rapamycin-insensitive mTORC2, when bound to Rictor.

mTORC1 phosphorylates its downstream S6 kinase (S6K), which in turn phosphorylates the ribosomal protein S6 and other factors involved in translation initiation and elongation, thus stimulating protein synthesis. TORC1 also activates eukaryotic translation initiation factor 4E (eIF4E) by phosphorylating the inhibitory eIF4E-binding proteins (4EBPs). Akt also promotes protein synthesis by phosphorylating and inactivating GSK3β, thus releasing the GSK3β-dependent inhibition of the eukaryotic translation initiation factor 2B (eIF2B) (*Miyazaki and Esser, 2009; Schoenfeld, 2010*) (Figure 2 and 3).

Mechanosensory regulation of protein synthesis has been introduced as a mechanism of mTOR activation that is independent of insulin-like growth factor (IGF)-1 (*Philp et al., 2011*). This can occur through high-force contractions during resistance exercise, which can disrupt the sarcolemma and increase the concentration of membrane phosphatidic acid (PA) through activation of phospholipidase D (PLD) (*Egan and Zierath, 2013; Yamada et al., 2012*). PA subsequently activates mTOR (*O'Neil et al., 2009*).

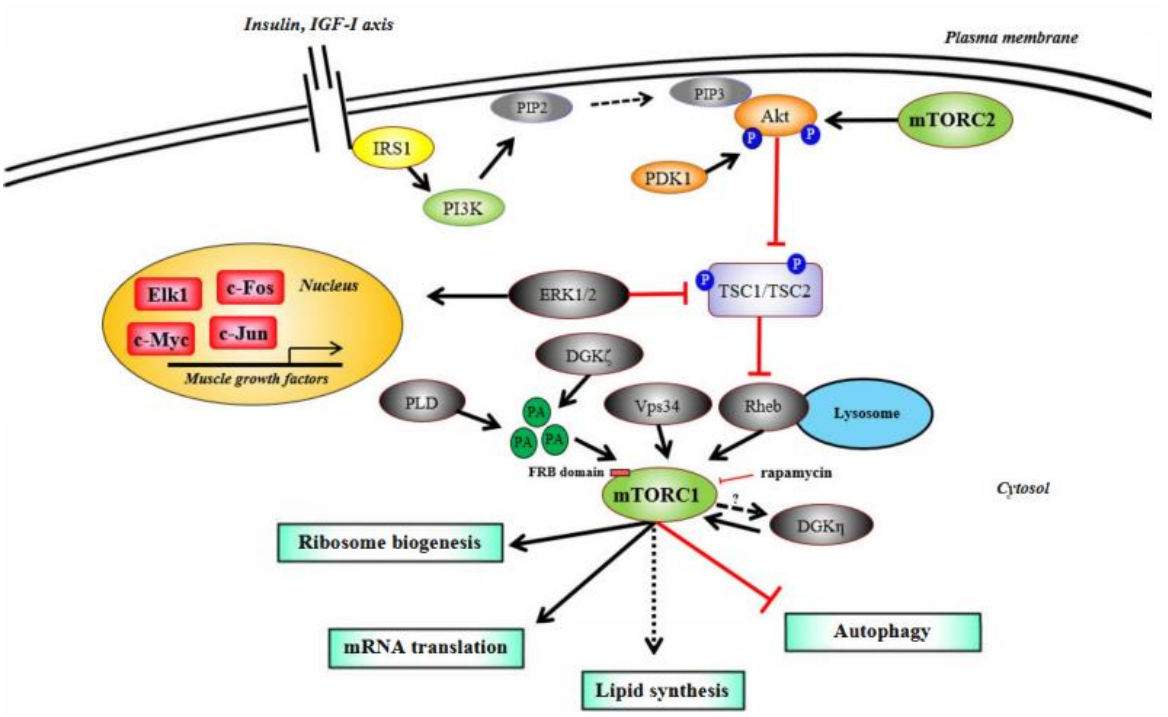


***Figure 2*** *mTORC1 regulates skeletal muscle protein synthesis. Upon IGF-1 (insulin-like growth factor 1) axis activation, IRS1 (insulin receptor substrate 1) activates the lipid kinase PI3K (phosphoinositide 3-kinase). PI3K phosphorylates the membrane bound phospholipid PIP2 (phosphatidylinositol diphosphate) and generates PIP3 (phosphatidylinositol triphosphate), which recruits Akt/PKB (protein kinase B) and PDK1 (phosphoinositide-dependent kinase-1). PDK1 phosphorylates and activates Akt, which then phosphorylates and inactivates*

*TSC1/TSC2 (tuberous sclerosis complex 1/2), a RHEB (Ras homolog enriched in brain) inhibitor. RHEB then activates mTOR (mechanistic/mammalian target of rapamycin) (from Solsona et al., 2021).*

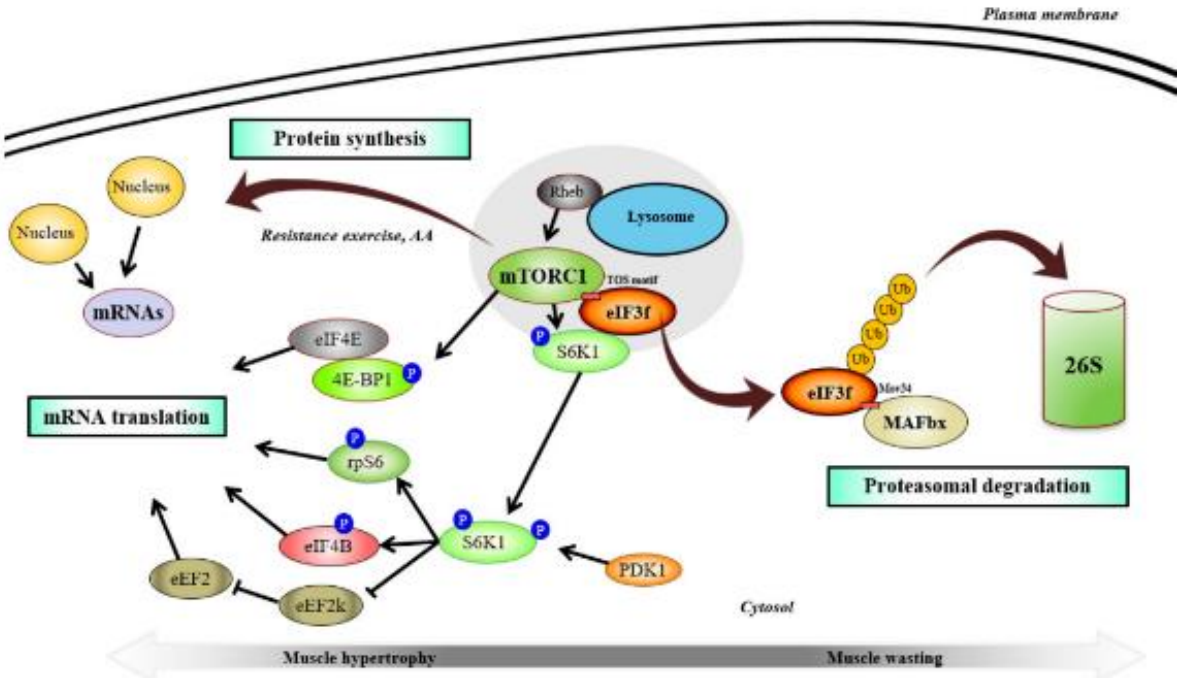


***Figure 3*** *mTORC1 regulates eIF3f in skeletal muscle protein translation. RHEB (Ras homolog enriched in brain) activates mTORC1 (mechanistic/mammalian target of rapamycin complex 1), which binds to the scaffold protein eIF3f (eukaryotic initiation factor 3f ) through a TOS (TOR signaling) motif and modulates mRNA translation by phosphorylating eIF3f bound- S6K1 (S6 kinase 1) and 4E-BP1 (eukaryotic translation initiation factor 4E-binding protein 1). S6K1-mediated regulation of translation occurs, in part, through phosphorylation of rpS6 (ribosomal protein S6), eIF4B (eukaryotic translation initiation factor 4B), and eEF2k (eukaryotic elongation factor-2 kinase). eEF2k inhibits eEF2 (eukaryotic elongation factor-2) to promotes mRNA translation. Phosphorylation of 4E-BP1 by mTOR (mechanistic/mammalian target of rapamycin) promotes its dissociation from eIF4E (eukaryotic initiation factor 4E) and allows for the assembly of the preinitiation complex. (from Solsona et al 2021).*

*Satellite cells* Satellite cells (SCs), also known as myogenic stem cells, reside in skeletal muscle between the basal lamina and the sarcolemma. Upon stimulation, SCs have the ability to drive out of their quiescent state to modulate their gene expression profile, and to start proliferating. These activated SCs termed myoblasts can stop their proliferation and differentiate into muscle progenitors (myocytes), which fuse with existing myofibers (*Vierck et al., 2000*). Fusion of myoblasts with pre-existent myofibers can lead to enhance myonuclear number (referred to “myonuclear accretion”) (*Goh et al., 2019*).

Whereas the role of SCs in fibre damage repair and remodeling is well described, SCs implication in muscle growth and hypertrophy has been debated for a long time in adult skeletal muscle. The increase in muscle proteins during muscle hypertrophy can be achieved either by increasing RNA and protein synthesis from existing nuclei or by maintaining the same level of RNA and protein synthesis from each nucleus and adding new nuclei to the fibres. Since the nuclei of adult muscle fibres

(myonuclei) are unable to divide, the new nuclei, which are incorporated by the fibre, come from outside the fibre. SCs are the main donors of new nuclei, being myogenic precursor cells that are important for muscle development, muscle regeneration, and possibly even muscle hypertrophy in response to exercise training (*Montarras et al., 2013*). They can fuse with existing muscle fibres, thereby contributing to the nuclei pool when there is an increased need for transcriptional activity (*Schiaffino and Reggiani, 1994*). SCs activation has been shown to occur during overload-induced muscle hypertrophy (*Schiaffino et al. 1972, 1976*), preceding hypertrophic growth (*Bruusgaard et al., 2010*).

Exercise is known to be an essential anabolic stimulus for muscle tissue, and it was shown that, according to the type of intervention, exercise modulates SCs activation for fibre repair or hypertrophy. The effect of resistance exercise on SCs activation is supported by numerous evidence and converge towards an increase in both SCs content and activation, as well as myonuclear accretion, a few hours after and until 4 days post-intervention (*Bazgir et al., 2016*).

### *Endurance training adaptations*

Endurance training is recognised to lead to improvements in cardiac output, maximal oxygen consumption, mitochondrial biogenesis, capillarization and fast-to-slow fibre-type transitions (*Smith et al., 2023*). These improvements in both the cardiovascular and musculoskeletal systems enable increased exercise capacity and performance (*Hughes et al., 2018*).

Endurance exercise training paradigms are commonly used to explore the phenotypic plasticity of mitochondria, which is one of the hallmark adaptations to endurance training. The mitochondrion is the main organelle for energy production through the generation of adenosine triphosphate (ATP) via the electron transport system (ETS), using substrates generated in the tricarboxylic acid (TCA) cycle (*Egan and Zierath, 2013; Bishop et al., 2014*).

*Mitochondrial biogenesis* Mitochondria contain their own DNA which encodes 13 subunits of the oxidative phosphorylation system. The remaining subunits, as well as other mitochondrial proteins, are encoded by the nucleus. Mitochondrial biogenesis depends on both the coordinated expression of the nuclear and mitochondrial genomes, the proper assembly of proteins encoded by these two genomes, and the

expression of proteins involved in the organisation of mitochondria into dynamic tubular networks.

Improved skeletal muscle oxidative capacity involves mitochondrial biogenesis through up-regulation of PGC-1α, which is a coactivator of transcription factors that has been identified as a master regulator of mitochondrial biogenesis and function. The downstream transcription factors of PGC-1α include nuclear respiratory factor-1/2 (NRF1, NRF-2) and mitochondrial transcription Factor A (mtTFA) (*Scarpulla et al., 2002*), supporting the notion that PGC-1α orchestrates mitochondrial biogenesis through the coordinated expression of transcripts encoded by either the mitochondrial or nuclear genomes (*Garnier et al., 2005*).

The activation of energy-sensing pathways during exercise promotes the induction of PGC-1α and mitochondrial biogenesis. The 5'-AMP-activated protein kinase (AMPK) is a cellular energetic sensor that is activated in response to low ATP and high AMP levels. This activation promotes mitochondrial biogenesis through the AMPK-PGC-1α axis (*Koulmann et al., 2006*). While there is evidence showing that AMPK activity is chronically increased with repeated exercise (*Frosing et al., 2004*), there are also observations that activation of AMPK in skeletal muscle fades with regular endurance training *(Nielsen et al., 1985; McConnell et al., 2005)*.

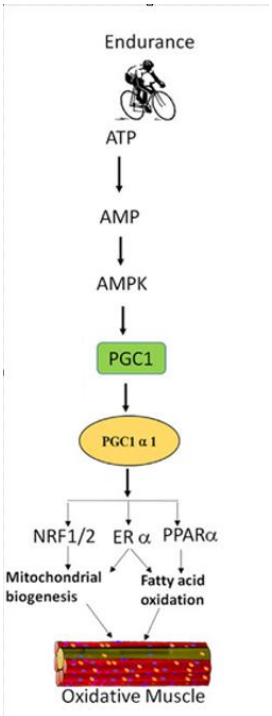


***Figure 4*** *Intracellular AMPK-PGC1a pathway triggered and endurance exercise (Qaisar et al., 2016).*

*Mitochondrial dynamics* Endurance exercise prompts mitochondrial morphological changes that augment the respiratory capacity of the worked muscles. Endurance training increases mitochondrial fusion protein levels in skeletal muscle, promoting the development of a hyperfused mitochondrial network (*Meinild Lundby et al., 2018)* (Figure 5). Mitochondrial fusion is the process of combining separate mitochondria to create elongated mitochondrial networks that promote oxidative phosphorylation (*Youle & van der Bliek, 2012*). The purpose of this process is to merge damaged mitochondria with healthy ones, preserving and optimizing mitochondrial function to meet high energy demands during cellular stress (*Chan, 2020*). The key molecular regulators of fusion are dynamin-related guanosine triphosphatases (GTPases), namely mitofusin 1 (Mfn1), mitofusin 2 (Mfn2) and optic atrophy 1 (Opa1) (*Chan, 2020)*. Mfn1 and Mfn2 bind the adjacent outer mitochondrial membranes (OMMs) together for fusion (*Ishihara et al., 2004*), while Opa1 regulates inner mitochondrial membrane (IMMs) fusion (*Youle & van der Bliek, 2012*). In contrast, mitochondrial fission is a process by which damaged or dysfunctional mitochondria are separated from the mitochondrial reticulum and targeted for mitophagy. Dynamin-binding protein 1 (Drp1) has been identified as the main regulator of mitochondrial fission (Figure 5). PGC-1α is also involved in mitochondrial network remodelling through controlled fusion and fission (*Cartoni et al., 2005*). Garnier ***et al***. also demonstrated that peak $VO_2$ in healthy humans was dependent on the coordinated expression of PGC-1α, which was linearly correlated with Mfn2 and Drp1 levels (*Garnier et al., 2005*). Other reports have shown that 12 weeks of endurance training increase the ratio of fusion-to-fission rates in human skeletal muscle (*Meinild Lundby et al., 2018)*. Additionally, OPA1 protein levels were found to be higher in the skeletal muscles of endurance-trained individuals (*Tezze et al., 2017; Marcangeli et al.,2022*). These findings suggest that a profusion environment arises in well-adapted muscles during exercise, likely to meet the higher energy demands (*Huertas et al., 2019*).

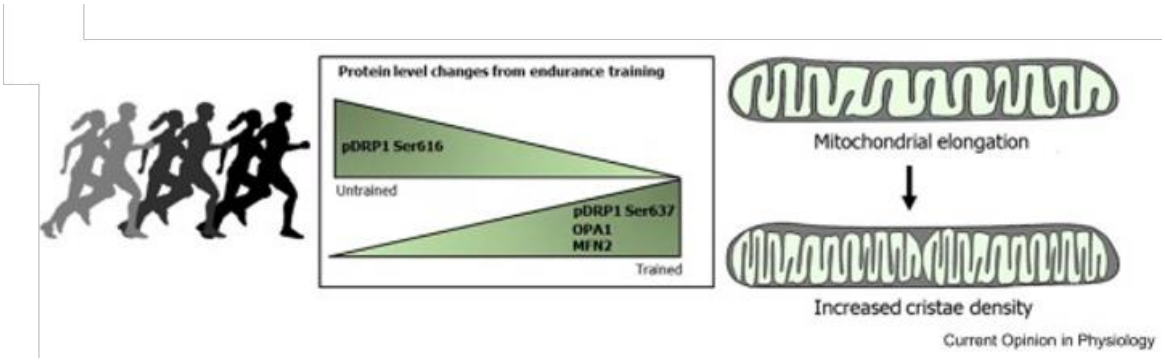


***Figure 5*** *Schematic representation of the changes in expression levels of fission and fusion proteins from long-term exercise training. As mitochondria become more resilient to exercise-incurred damage, fission activity is dampened, demonstrated by concomitant drops in DRP1 phosphorylation on Ser616 and increases in DRP1 phosphorylation on Ser637. Additionally, MFN2 and OPA1 levels increase. Overriding fusion rates lead to an expansion of the mitochondrial network to enhance the oxidative capacity of the trained muscles.*

*Fibre type transition* It is well known that endurance exercise promotes phenotypic adaptations in skeletal muscle toward a more oxidative phenotype (from fast-twitch muscle fibre to slow-twitch muscle fibre) (*Andersen et al., 1977*).

Calcium acts as a second messenger in skeletal muscle, and evidence suggests that calcium signalling and handling play a crucial role in determining muscle fibre types. Calcium-triggered regulatory pathways, acting through (1) calcineurin, (2) $Ca^{2+}$–calmodulin-dependent protein kinases (CaMK), (3) and $Ca^{2+}$-dependent protein kinase C, are involved in determining muscle phenotype (*Koulmann et al., 2006*) (Figure 6). Calcineurin may be activated by prolonged endurance exercise in human skeletal muscle (*Norrbom et al., 2004*), supporting its role in the training-induced alterations of muscle phenotype. A significant interaction exists between PGC-1α and calcineurin during physical exercise. It has been suggested that PGC-1α could be a physiological regulator that integrates calcineurin signalling, mitochondrial biogenesis, and myofibrillar protein regulation (*Koulmann et al., 2006*). This hypothesis is consistent with the role of PGC-1α in activating the expression of myofibrillar proteins that are characteristic of type I fibres. In addition to calcineurin, PGC-1α expression is also responsive to the p38 MAPK pathway and CaMKs activity (Figure 6) (*Koulmann et al., 2006*). These findings link the control of the slow contractile phenotype to the regulation of oxidative metabolism, ensuring a strong coordination of the expression of both contractile and metabolic proteins within myofibres.

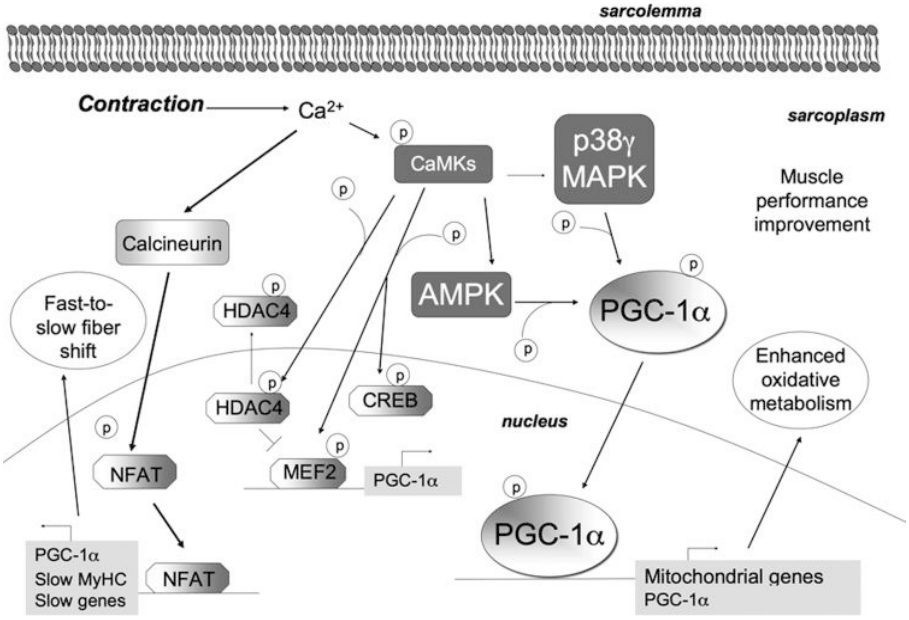


***Figure 6*** *Exercise adaptation is mediated by Ca2+ signaling. During exercise, Ca2+ concentration increases inside the myofiber and activates CaMKs. Calcineurin is a phosphatase that primarily dephosphorylates and activates NFAT. NFAT mainly promotes the transcription of PGC-1α and slow genes (such as MyHC), thus most probably mediating the fast-to-slow myofiber transition. CaMKII is the main isoform of CaMKs in human skeletal muscle. On Ca2+ increase due to exercise, CaMKs become phosphorylated in an intensity-dependent manner; they, along with p38 MAPK, target PGC-1α and mitochondrial biogenesis. In addition, CaMKs might also phosphorylate cAMP-response element Binding Protein (CREB), AMPK, and (Histone deacetylases) HDACs. CaMKs phosphorylate and directly active MEF2, which promotes the transcription of PGC-1α nuclear HDAC4 inhibits MEF2. By phosphorylating HDAC4, CaMKs induce HDAC4 export out of the nucleus, thereby releasing MEF2. CaMKs, Ca2+/calmodulin-dependent kinases; NFAT, nuclear factor of activated T-cells (Feraro et al., 2014).*

*Capillarization* The increase in capillary supply in skeletal muscle in response to exercise results in greater diffusive exchange of oxygen ($O_2$), nutrients, and extraction of metabolic waste compounds (carbon dioxide [$CO_2$], ammonia, lactate). Skeletal muscle angiogenesis is highly regulated by exercise (*Gute et al. 1996; Prior et al., 2004)* (Figure 7), and enhanced muscle capillarization can result in benefits for endurance performance, as well as improvements in cardiovascular and skeletal muscle health.

The main mediator of increased capillarization with endurance exercise is the vascular endothelial growth factor A (VEGF), which influences several steps in angiogenesis, including the activation, proliferation, and migration of endothelial cells (*Ferrara, 1999*). VEGF protein is present in various cells in the muscle, including skeletal muscle myofibers, pericytes (*Hoier et al. 2013b*), and endothelial cells (*Milkiewicz et al. 2001*). At the transcriptional level, VEGF is induced by hypoxia-inducible factor (HIF)-1α and estrogen-related receptor α (ERRα) via PGC-1β and PGC-1α. These are transcription factors that also regulate other oxidative aspects,

including mitochondrial biogenesis, suggesting a coordinated metabolically coupled regulation (*Ross et al., 2023*).

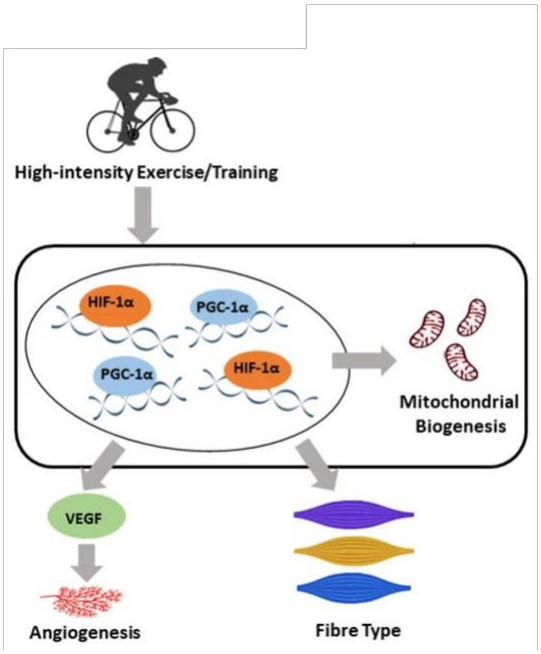


***Figure 7*** *A model for the molecular adaptive responses of skeletal muscle to high-intensity exercise/training. Exercise/training induces a range of adaptations, including an upregulation in angiogenesis and mitochondrial biogenesis and a shift in the skeletal muscle fibre type. Peroxisome proliferator-activated receptor gamma coactivator 1 alpha (PGC-1α), hypoxia-inducible factor 1-alpha (HIF-1α), and vascular endothelial growth factor (VEGF) play important roles in the regulation of the adaptive response to high-intensity exercise/training within skeletal muscle (Li et al., 2020).*

### *Skeletal muscle memory and exercise*

Skeletal muscle memory has been defined as "*the ability of the skeletal muscle to respond differentially to environmental stimuli, either adaptively or maladaptively if the stimuli have been encountered previously" (Sharples et al., 2016b)*. This definition encompasses both cellular and tissue retention of preceding environmental stimuli or stress, such as those derived from acute or chronic exercise, muscle damage/injury, disease, and nutrition changes. Skeletal muscle is greatly affected by its environment. An anabolic/positive environment can lead to incremental muscle growth or maintenance of good health over a lifetime. Conversely, a catabolic/negative environment can make skeletal muscle more susceptible to loss of muscle mass later in life.

*Skeletal muscle memory and resistance training* Some studies have shown that muscle fibres may possess a form of cellular memory, which may explain why previously acquired muscle mass is more easily recovered. The cellular mechanism

of this process is associated with the number of myonuclei acquired during overload (*Bruusgaard et al., 2010; Egner et al., 2013; Gundersen, 2011*).

Bruusgaard and colleagues proposed a model (Figure 8A-B) based on the observation that myonuclei acquired by overload exercise precede hypertrophy and are not lost on detraining. According to this model, previously untrained fibres acquire new nuclei by fusion of satellite cells preceding the hypertrophy when subjected to a hypertrophic stimulus. Atrophy occurs during subsequent detraining, but no loss of myonuclei is observed. If retrained, such fibre would hypertrophy without recruiting new nuclei, and this retraining route would be faster than the first training route (*Burrsgaard et al., 2010*).

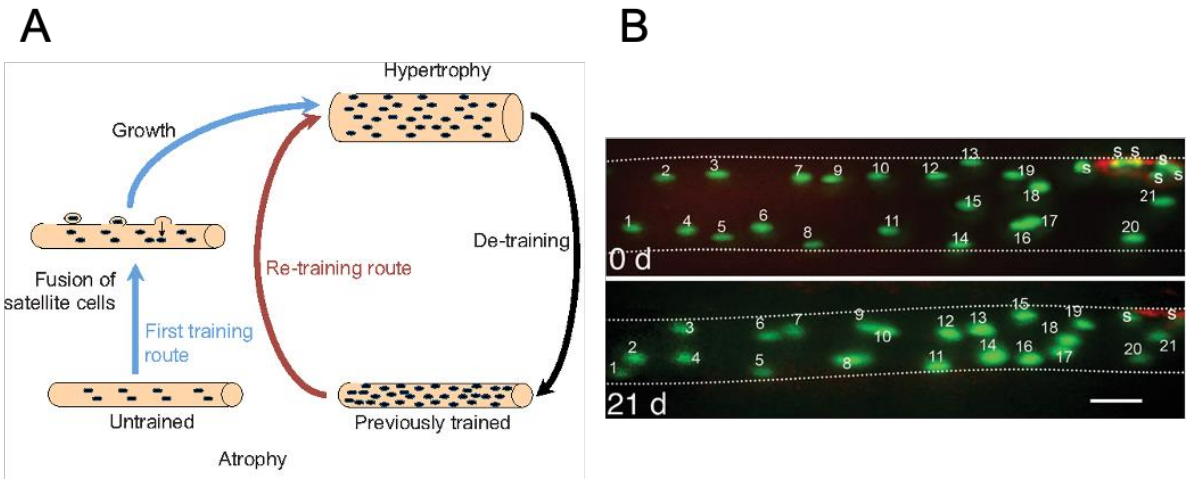


***Figure 8 A**) New model for the cell biology of hypertrophy and atrophy. For naïve fibres and preceding hypertrophic growth, myonuclei are recruited from satellite cells, temporarily reducing the myonuclear domain volume, leading to a large fibre with many myonuclei. Upon subsequent atrophy, the myonuclei are maintained, leading to a small fibre with a high myonuclear density and small myonuclear domains. Such fibres can hypertrophy without recruiting new nuclei, and this retraining route seems to be faster than the first training route. The permanently higher number of myonuclei represents the muscle memory. Adapted from Bruusgaard et al. (2010). **B**) Myonuclei are not lost during atrophy. Time-lapse in vivo imaging of the same fibre segment before (day 0) and after 21 days of denervation. Note that the number of nuclei in the segment left of the neuromuscular endplate labelled in red is the same despite the pronounced atrophy. Scale bar, 50 µm. Adapted from Gundersen and Bruusgaard (2008).*

Some evidence supports this model. For example, a 2-weeks treatment with testosterone in mice resulted in an increase in fibre size and number of nuclei (*Egner et al., 2013*). Three weeks after discontinuing the drug, fibre size had returned to normal, but the number of nuclei remained constant and high for at least 3 months. When overloaded, muscles grow more and faster (*Egner et al., 2013*).

Similar effects were observed in trained animals. During the 8-week resistance training period myonuclei increased and were maintained throughout the 20-week detraining period. Relative muscle mass improved even more after repeating the second training period compared to the first (*Lee et al., 2018*). Additionally, the study showed that mitochondria markers respond more consistently to repeated, non-

continuous resistance training interventions. This finding suggests the possible existence of a memory mechanism for specific aerobic physiological markers.

The existence of this phenomenon has not been well established in humans. Recent studies in humans have shown that acquired myonuclei are not resistant to longer periods of inactivity and return to the untrained state after training cessation (*Murach et al., 2019; Psilander et al., 2019; Snijders et al., 2019*). This challenges the concept of muscle memory based solely on the number of myonuclei in the long-term and suggests alternative mechanisms for muscle memory *(Seaborne et al., 2018a; Turner et al., 2019).*

The role of epigenetics has also emerged as another important mechanism involved in muscle memory, enabling muscles to "remember" previous exercise. Upstream signalling, along with an altered intramuscular metabolic milieu, can change the chromatin landscape in muscle, and thus influence transcription factor-driven gene expression in response to exercise (*Smith et al., 2023*) (Figure 9). Epigenetic modifications to amino acids in histone tails or globular core domains can create a permissive or repressive chromatin state, depending on the type of modification and the targeted residue and/or histone protein (*Smith et al., 2023*). DNA methylation and histone modifications are the most significant epigenetic changes described in gene transcription. They are linked to the skeletal muscle transcriptional response to exercise and mediate the exercise adaptations. DNA methylation is the process of adding a methyl group to cytosines within CpG dinucleotides, resulting in the formation of 5-methylcytosine (5-mC). This process is carried out by specific DNA methyltransferases (DNMTs) (Meier and Recillas-Targa, 2017), and is often associated with gene silencing. Seaborne and colleagues were the first to demonstrate this phenomenon in humans (*Seaborne et al., 2018a*). They found that repeated resistance training interventions led to a greater increase in lower limb lean mass compared to the previous training stimulus. This pattern was accompanied by epigenetic modifications (via DNA methylation) characterized by retention of hypomethylation acquired during initial training even during the detraining period or followed by larger hypomethylation after later retraining (*Seaborne et al., 2018a)*. These signatures were associated with an enhanced expression of targeted genes, allowing for an improved molecular response to repeated resistance training.

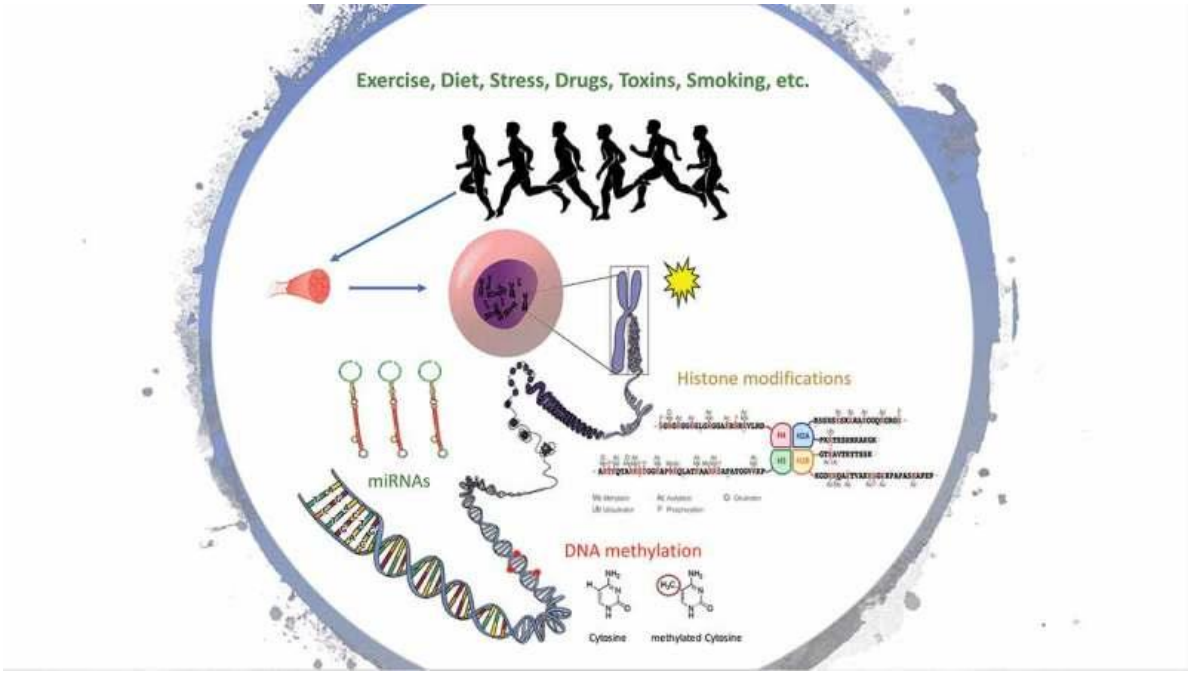


***Figure 9*** *DNA methylation in response to different environmental stimuli (Jacques et al., 2019).*

*Epigenetics adaptations in response to endurance exercise* There is evidence indicating that epigenetics play a role in skeletal muscle adaptation to endurance training. Studies have shown that regular endurance exercise in human is associated with changes in DNA methylation in skeletal muscle, specifically in genes related to muscle growth, differentiation, and metabolism (*Niert et al., 2012*). Similar findings have been observed in trained mice (*Kanzleiter et al., 2015*). Furthermore, Lindholm and colleagues demonstrated that a three-month endurance training program of a single-leg resulted in changes in the methylation patterns of genes related to myogenesis, muscle structure and muscle bioenergetics. The analysis of gene expression at the transcriptome level, along with the analysis of methylation at the genome level, revealed significant correlations between changes in DNA methylation and changes in gene expression. Correlations were observed in groups where there was a decrease in methylation and a concomitant increase in expression, or vice versa (*Lindholm et al., 2014*).

The PGC-1α gene is one of the most well-characterised genes that is upregulated in response to endurance exercise. Studies in both humans (*Barrès et al., 2012*) and mice (*Laker et al., 2014; Lochmann et al., 2015*) have shown that following exercise, this gene appears to be demethylated within its promoter sequence. Demethylation can be observed both after acute training (*Barrès et al., 2012, Lochmann et al., 2015*) and after a 6-week voluntary running protocol (*Laker et al., 2014*). Barrès and

colleagues (*Barrès et al., 2012*) showed that high-intensity exercise (80% $VO_{2max}$) immediately reduced methylation levels in the promoter regions of *PGC1α*, *PDK4*, and *PPARδ* in human skeletal muscle, which was associated with increased transcription of these genes. Notably, the same exercise performed at a lower intensity (40% $VO_{2max}$) did not have an impact on DNA methylation. This suggests that exercise intensity may be a critical factor in influencing DNA methylation.

Currently, there has been limited research on a possible mechanism of skeletal muscle memory triggered by aerobic training in humans. Only one study has explored the potential presence of transcriptional memory in skeletal muscle following repeated endurance training (*Lindholm et al., 2016*). The participants underwent two 12-week periods of moderate-intensity, single-leg aerobic training, with a 9-month detraining period between them. The authors did not find evidence to support of the presence of a transcriptomic memory. In fact, no retention of gene expression profiles was observed during the detraining period, and even functional endurance adaptation was not different between the two training interventions.

However, the question remains unanswered. As described above, exercise intensity is a crucial factor in influencing DNA methylation. Methylation and gene expression involved in metabolic and oxidative pathways are more affected by high-intensity exercise than by moderate-intensity exercise *(Barrès et al., 2012).*

### *High-Intensity Interval Training*

High-intensity interval training (HIIT) is a powerful stimulus that affects the content, localisation, and/or activity of nuclear proteins and genes coding for mitochondrial proteins in a short period. HIIT is characterised by short bursts of relatively intense exercise interspersed with recovery periods within a given training session. It is, therefore, possible to stimulate rapid adaptations in skeletal muscle comparable to traditional endurance training with a relatively small dose of HIIT, provided the exercise stimulus is very intense and applied intermittently (*Gibala et al. 2006; Burgomaster et al. 2008*).

HIIT has been shown to stimulate mitochondrial biogenesis in skeletal muscle, leading to remodelling towards a more oxidative phenotype and improved metabolic health markers (*TjØnna et al., 2008; WislØff et al., 2007; Batterson et al., 2023*). Additionally, HIIT has been found to induce a larger, more fused mitochondrial tubular network (*Ruegsegger et al., 2023*). Changes indicating increased fusion following

HIIT are associated with improvements in mitochondrial respiration and $VO_{2peak}$, supporting the idea that enhanced mitochondrial fusion accompanies notable health benefits of HIIT (*Ruegsegger et al., 2023*).

Therefore, this training mode appears promising for investigating the presence of muscle memory triggered by aerobic exercise.

## RATIONALE AND AIM

The rationale for this study is supported by several observations:

- an initial exposure to a hypertrophic stimulus, such as resistance exercise, leads to faster and greater skeletal muscle growth when the muscle is exposed to the same stimulus following a period of detraining. This led to the concept of muscle memory, whose mechanism appears to be mediated by the permanent retention of myonuclei acquired during the initial phase of hypertrophic growth.
- The role of epigenetics has emerged as another important mechanism involved in resistance exercise-induced muscle memory. This mechanism is based on a long-term DNA hypomethylation 'memory' of prior exercise training, that could have consequences for future adaptability of myofibres during retraining.
- Acute high-intensity endurance exercise has been shown to promote epigenetic modifications resulting in increased gene expression of mitochondrial biomarkers. Therefore, in principle, chronic high-intensity endurance exercise may trigger muscle memory processes.
- It is currently unclear whether oxidative metabolism and mitochondrial function adapt to repeated high-intensity endurance training interventions and retain adaptations over time.
- Mitochondrial dysfunction is associated with various pathological conditions, including metabolic disorders, neurodegenerative diseases, and aging. Understanding the positive impact of repeated aerobic exercise on mitochondrial function and its long-term retention could have significant implications for preventing or managing these conditions.

Based on these observations, the aim of this project is to investigate the presence of muscle memory in response to two repeated high-intensity interval training interventions, separated by a period of long-term detraining.

## MATERIALS AND METHODS

### *Participants*

Twenty adult participants (11 male and 9 female) (age 25 ± 5 years; weight 66.1 ± 11.4 Kg; height 173 ± 7 cm) were recruited. Inclusion criteria required that participants had no prior experience with structured training programs. Additionally, aerobically fit individuals ($VO_{2\ peak}$ > 45 $ml \cdot min^{-1} \cdot kg^{-1}$) were excluded based on the initial screening test. All participants completed a health history questionnaire to ensure the absence of chronic disease. Prior to enrolment, participants were informed of the aims, methods, and risks and provided written consent. All procedures were in accordance with the Declaration of Helsinki and study was approved by the local ethics committee (Besta 64-19/07/2019).

| | **Age (years)** | **Weight (kg)** | **Height (cm)** | $\dot{V}O_{2peak}$ **($ml \cdot min^{-1} \cdot kg^{-1}$)** | $\dot{V}O_{2peak}$ **($l \cdot min^{-1}$)** |
|---|---|---|---|---|---|
| Males (n=11) | 27 ± 5 | 72.1 ± 10.7 | 177 ± 5 | 36.8 ± 8.3 | 2.601 ± 0.448 |
| Females (n=9) | 23 ± 3 | 58.7 ± 7.2 | 167 ± 4 | 34.1 ± 5.3 | 1.985 ± 0.308 |

***Table 1*** *Participants anthropometric and physiological characteristics measured during the initial screening test grouped according to sex $VO_{2PEAK}$, peak oxygen uptake. All values are means ± SD.*

### *Study design*

The current study exposed the same individuals to two identical 8-week interval training periods separated by a three-month washout period of detraining, during which participants were instructed to return to their pre-study levels of physical activity. Measurements were taken at four different time points: at baseline (BASELINE), after the first training period (TRAINING), following detraining (DETRAINING) and after the second training period (RETRAINING).

For each time point, participants visited the laboratory on two separate occasions. During the first visit of testing, anthropometric measurements were taken and a cycle incremental cardiopulmonary exercise test to the limit of tolerance was performed to determine $\dot{V}O_{2peak}$ and gas exchange threshold (GET). Forty-eight hours after incremental exercise the second visit was arranged where approximately 100 mg of skeletal muscle was obtained from the *vastus lateralis* muscle by percutaneous conchotome under local anesthesia (1% lidocaine). Following training periods, the two visits were performed 48 hours after the final training session. Participants were

instructed to abstain from strenuous physical activity for at least 24 hours prior to each testing session (48 hours for the biopsy trial).

### *Training*

Training consisted of two identical 8-week periods separated by a three-month wash-out period. During both training and retraining, participants trained independently three times per week with interval training sessions on electronically braked cycle ergometer (Nowa, Diadora, Italia) for a total of 24 training sessions for each period. Interval training involved high-intensity interval training (HIIT), in both low-volume (interval duration ≤ 2 minutes) and high-volume (interval duration > 2 minutes), and sprint interval training (SIT). To avoid stagnation, the training stimulus of high-intensity intervals was progressively incremented in subsequent training sessions by increasing the relative exercise intensity and repetitions (*Granata et al., 2016a*).
Overall, each training period consisted of the following different training exercise modalities. 1) Four training sessions were composed of 4 min of cycling intervals interspersed with 2 min of recovery at 30–50% $W_{GET}$. Training intensities were defined as $W_{GET} + x (W_{peak} – W_{GET})$, where x = 0.35, 0.50, 0.65, and 0.75 for sessions 1- 4, respectively. Number of repetitions was 4, 5, 6 and 6 for sessions 1–4, respectively. 2) Two training sessions comprising 10 bouts of 2-min cycling intervals interspersed with 1-min recovery at 30– 50% $W_{GET}$. Training intensities in the two sessions were defined as $W_{GET} + x (W_{peak} – W_{GET})$, where x = 0.8 and 0.9, respectively. 3) Three training sessions were structured with 1-min cycling intervals interspersed with 2 min of recovery at 30–50% $W_{GET}$. Training intensities were defined as 100, 110, and 120% of $W_{PEAK}$ for sessions 1–3, respectively. Number of repetitions was 6, 8 and 10 for sessions 1–3, respectively. 4) Three training sessions consisted of “all-out” 30-second cycle sprint interspersed with 4 min of self-managed recovery. Repetitions were 6, 7, and 8 for sessions 1–3, respectively. During this training mode cycle, the ergometer was set in hyperbolic mode with a resistance that allowed to elicit the power of 170% $W_{peak}$ with 80 rpm and participants were instructed to pedal as faster as possible. Exercises were alternated during the training period to facilitate participant motivation and compliance, as detailed previously (*Robach et al., 2014*). An identical training protocol was applied for both training and retraining periods.

### *Incremental exercise*

Power during step-incremental cycling was increased 10-15 W every minute, depending on the individual's fitness. Participants were instructed to maintain constant cadence at their preferred value (between 70 and 85 rpm). Intolerance was defined when participants could no longer maintain their chosen pedaling frequency despite verbal encouragement.

Pulmonary ventilation ($V_E$, in BTPS [body temperature (37°C), ambient pressure and gas saturated with water vapour]), oxygen consumption ($VO_2$), and $CO_2$ output ($VCO_2$), both in STPD (standard temperature [0°C or 273 K] and pressure [760 mmHg] and dry [no water vapour]), were determined breath-by-breath by a metabolic cart (Vyntus CPX, Vyaire Medical GmbH, Germany). Before each test, gas analyzers were calibrated with ambient air and a gas mixture of known concentration ($O_2$: 16%, $CO_2$: 4%) and the turbine flowmeter was calibrated with a 3-L syringe at three different flow rates. RER was calculated as $VCO_2/VO_2$. HR was recorded by using an HR chest band (HRM-Dual, Garmin, Kansas, USA). Rating of perceived exertion (RPE) was determined using Borg® 6–20 scale every 2 min through the test (Borg, 1982). At rest, and at 1, 3, and 5 min of recovery, 20 µL of capillary blood was obtained from a preheated earlobe for blood lactate concentration (Biosen C-line, EKF, Germany); the analyser was frequently calibrated with a standard solution containing 12 mmol·L−1 of lactate. Peak cardiopulmonary variables were measured from the highest 20 s mean values before intolerance when at least two of the following criteria were found: 1) maximal levels (>15) of RPE; 2) HR values higher than 85% of the age-predicted maximum; 3) RER values equal or above 1.1; and 4) $[La]_b$ during recovery higher than 8 $mmol \cdot L^{-1}$. Peak values were further verified after 30 min of recovery by means of a supramaximal verification trial performed at 90% of peak power output ($W_{peak}$). GET was determined by two independent investigators by using the modified "V-slope" method (*Beaver et al., 1986*) and "secondary criteria". The power at GET was estimated after accounting for the individual's $\dot{V}O_2$ mean response time (*Whipp et al., 1981*).

### *Muscle Biopsy*

Fifteen participants of 20 (9 male and 6 female) (age 24 ± 5 years; weight 65.8 ± 12.1 kg; height 173 ± 5 cm) underwent to a muscle biopsy for all the time points required by the experimental protocol. Approximately 100 mg of tissue were collected. Resting

muscle biopsies were taken from the *vastus lateralis* muscle using a 130 mm (6'') Weil-Blakesley rongeur conchotome (NDB-2, Fehling Instruments, GmbH & Co, Germany) under local anaesthesia (1% lidocaine) of skin and muscle fascia. A 1.0 – 1.5 cm incision was made to the skin, subcutaneous tissue and muscle fascia, and the tissue sample was harvested. After collection, muscle samples were cleaned of excess blood, fat, and connective tissue and were divided into four parts for different analyses. A portion of ~20 mg of muscle tissue was immediately submerged in All Protect Tissue Reagent (Qiagen, Netherlands) following the manufacturer's instructions to stabilise and protect cellular DNA and RNA and was stored at -20°C for subsequent DNA methylome analysis. A specimen of ~20-30 mg was rapidly frozen by immersion in liquid nitrogen and stored at -80°C for gene expression analysis. A portion of ~10-20 mg of each muscle sample was placed in a plate containing ice-cold preservation solution (BIOPS; Oroboros Instruments, Innsbruck, Austria) (4°C) containing: (2.77 mM CaK2EGTA, 7.23 mM K2EGTA, 5.77 mM Na2ATP, 6.56 mM $MgCl_2$, 20 mM taurine, 50 mM MES (2-(N-morpholino)ethane-sulfonic acid), 15 mM Na2phosphocreatine, 20 mM imidazole, and 0.5 mM dithiothreitol adjusted to pH 7.1) and immediately used for high-resolution respirometry (HRR) analysis. A portion of ~20/30 mg from each muscle sample was rapidly frozen by immersion in liquid nitrogen and stored at -80°C for proteomic analysis. The remaining portion was included in optimal cutting temperature (OCT, Tissue-Tek, Sakura Finetek Europe, The Netherlands) embedding medium, frozen in iso-pentane, cooled down on liquid nitrogen, and used for histological stains and Cross-Sectional Area (CSA) determinations.

### *High-Resolution Respirometry*

For high-resolution respirometry (HRR) analysis, muscle fibres were trimmed from the connective and fat tissue excess (if present) and mechanically separated with pointed forceps in an ice-cold BIOPS buffer. The plasma membrane was permeabilized by gentle agitation for 30 min at 4°C in 2 mL of BIOPS buffer containing 20 $\mu g \cdot mL^{-1}$ saponin and was followed by 10 min washing in MiR05, a respiration medium containing 0.5 mM EGTA, 3 mM $MgCl_2$, 60 mM lactobionic acid, 20 mM taurine, 10 mM $KH_2PO_4$, 20 mM HEPES (4-(2- hydroxyethyl)piperazine-1-ethane sulfonic acid), 110 mM D-sucrose, and 1 $g \cdot L^{-1}$ bovine serum albumin (BSA), essentially fatty acid-free (pH 7.1) (*Pesta & Gnaiger, 2012*). Permeabilized fibres

were weighed. Mitochondrial respiration was evaluated by measuring $O_2$ flux ($JO_2$) polarographically (*Pesta & Gnaiger, 2012*). The analysis was performed in duplicate (from 3 to 6 mg wet of muscle fibres) in 2 mL of MiR05 at 37°C containing myosin II-ATPase inhibitor (25 µM blebbistatin dissolved in DMSO 5 mM stock) to inhibit contraction (*Perry et al., 2011*), using the high-resolution Oxygraph-2k (Oroboros, Austria). Oxygen concentration and flux were recorded using DatLab4 software (Oroboros Instruments, Austria). Polarographic $JO_2$ measurements were acquired at 2 s intervals with the steady-state rate of respiration calculated from a minimum of 40 data points and expressed as $pmol \cdot s^{-1} \cdot mg^{-1}$ wet wt. Chamber $O_2$ concentration was maintained between 250 and 450 $nmol \cdot mL^{-1}$ (average $O_2$ partial pressure 250 mmHg) to avoid $O_2$ limitation of respiration (*Pesta & Gnaiger, 2012*). Standardized instrumental and chemical calibrations were performed to correct for back-diffusion of $O_2$ into the chamber from the various components (e.g., leak from the exterior, $O_2$ consumption by the chemical medium, and by the $O_2$ sensor) (*Pesta & Gnaiger, 2012*).

A substrate-uncoupler-inhibitor titration protocol (SUIT) was used (*Pesta & Gnaiger, 2012*). Glutamate (10 mm) and Malate (4 mm) were added to assess LEAK respiration through complex I ($CI_L$). Submaximal titration of ADP (2.5, 5,10, 25, 50, 100, 175, 250, 500, 1,000, 2,000, 4,000, 6,000, 8,000, and 10,000 µM) was added to measure the ADP sensitivity sustained by complex I. Apparent $K_m$ ([ADP]) providing 50% of the maximum mass-specific oxygen flux ($JO_2$) was calculated by using a Michaelis–Menten kinetic equation (*Zuccarelli et al., 2021*). ADP (10 mm) was added to assess maximal oxidative phosphorylation (OXPHOS) capacity through CI ($CI_P$). Succinate (10 mm) was added to assess OXPHOS capacity through CI + complex II ($CI + II_P$). Cytochrome c (10 µm) was added to test for outer mitochondrial membrane integrity. Stepwise additions of carbonyl cyanide p-trifluoromethoxyphe-nylhydrazone (FCCP; 0.5–1.5 µm) were used to measure electron transport system (ETS) capacity through CI+II ($CI+II_E$). Inhibition of CI by rotenone (1 µm) determined electron transport system capacity through CII ($CII_E$), whereas addition of antimycin A (2.5 µm), inhibitor of complex III, was used to measure residual oxygen consumption, which was subtracted from all measurements. The respiratory control rates (RCR) were measured as indicators of the mitochondrial coupling state ($RCR=CI_P/CI_L$ ratio). Results were expressed in $pmol \cdot s^{-1} \cdot mg^{-1}$ wet calculating mean values of duplicate analyses. At the conclusion of each experiment, muscle samples were removed from

the chamber, immediately frozen in liquid nitrogen, and then stored at -80°C until measurement of citrate synthase (CS) activity.

### *Citrate Synthase Activity*

CS activity was determined by using the Citrate Synthase Activity Assay kit (Merck, Darmstadt, Germany). Muscle samples were homogenized in an ice-cold CS Assay Buffer provided by the kit, kept on ice for 40 min, and centrifuged at 10,000 g for 20 minutes at 4°C to obtain a protein extract. Protein concentration was then determined using the RC-DC protein assay (Bio-Rad, Hercules, CA), and 5 µg of protein lysate was used to test CS activity. After adding the appropriate Reaction Mix, the absorbance was measured at 412 nm at the initial time ($T_{initial}$) with a plate Reader (CLARIOstar Plus, BMG Labtech, Germany) and then the reaction was followed for 45 min taking an absorbance measurement ($A_{412}$) every 5 min. CS enzyme activity was calculated by interpolating the reading at the final time ($T_{final}$) on a standard curve whose points were scalar concentrations of a solution of known concentration (2 nmol/µL) of GSH Standard solution.

*Protein Analysis*<u>*Sample preparation: muscle lysis and protein extraction*</u> Frozen muscles were pulverized in a steel mortar using a ceramic pestle, with the constant addition of liquid nitrogen to maintain muscle components' properties. The powder obtained was homogenized with a lysis buffer containing TRIS-HCl 20 mM, Triton 100x 1%, Glycerol 10%, NaCl 150 mM, EDTA 5 mM, NaF 100 mM and NaPPi 2 mM supplemented with protease inhibitors 5x (Protease Inhibitor Cocktail, Sigma-Aldrich, St. Louis MO), phosphate inhibitors 1x (Protease inhibitor Cocktail, Sigma-Aldrich, St. Louis MO) and Phenylmethylsulfonyl fluoride (PMFS) 1 mM. Tissue lysis was performed on ice for 40 min. The homogenate obtained was centrifuged at 13,500 rpm for 20 min at 4°C and the supernatant was transferred to clean Eppendorf tubes and stored at -80°C until use.

The protein concentration of the lysates was determined using the reducing agent and detergent compatible (RC-DC™) protein assay (Bio-Rad, Hercules, California, USA) which is a colorimetric assay for protein determination in the presence of reducing agents and detergents.

<u>*Western Blot*</u> Equal amounts of muscle samples were loaded on 4-20% gradient precast gels purchased from BioRad (Bio-Rad, Hercules, California, USA) and

subjected to electrophoresis. Electrophoresis run was carried out at constant current (100 V) for about ~2 h in a running buffer at pH 8.8 (Tris 25 mM, Glicine 192 mM, SDS 1%). To monitor protein separation, a protein molecular weight marker constituted by a mixture of proteins with known molecular weight (Prestained Protein Ladder Marker, Bio-Rad, Hercules, California, USA) was loaded on the gel.

Proteins were electro-transferred to polyvinylidene fluoride (PVDF) membranes at constant voltage at 100 V for two hours in a transfer buffer containing Tris 25 mM, Glycine 192 mM, and methanol 20%. The effective protein transfer to the membrane was verified by staining with Ponceau Red (Merck, Darmstadt, Germany) in acetic acid (Ponceau Red 0.2% in acetic acid 3%) for 15 min under stirring at room temperature.

Nonspecific binding sites present on the PVDF membrane were saturated with a blocking solution consisting of 5% fat-free milk in solution with Tris 0.02 M, NaCl 0.05 M and Tween-20 0.1% (Tris-buffered saline-Tween 20, TBS-T) for 2 h at room temperature with constant shaking. At the end of incubation, the membrane was washed with TBS-T for three times 10 min each. After that, the membranes were probed with specific primary antibodies (Table 2) overnight at 4°C. Thereafter, the membranes were incubated in appropriate horseradish peroxidase (HRP)-conjugated secondary antibodies.

Proteins detection was made using an enhanced chemiluminescence advance detection system (GE Healthcare Life Sciences, Little Chalfont, UK) that highlights the horseradish peroxidase (HRP) substrate by a chemiluminescent reaction. The membrane was gained through an analysis software ImageQuant LAS 4000 (GE Healthcare Life Sciences, Little Chalfont, UK). The content of each protein investigated was assessed by determining the brightness-area product of the protein band as previously described (*Cannavino et al., 2014*). The target protein levels were then normalized to total proteins in lysates by Ponceau stain or evaluated between phosphorylated and unphosphorylated total forms of the same protein (*Brocca et al., 2017*).

| TARGET PROTEIN | PROTEIN LYSATE (ug) | TRANSFER TIME | BLOCK SOLUTION | AB I | COMPANY | AB II | COMPANY |
|---|---|---|---|---|---|---|---|
| **p-AMPK** | 40 | 100 V 2h | 5% milk 2h RT | 1:1000 5% BSA O/N | Cell signalling | Anti-rabbit (1:1000) milk 5% | Cell signalling |

| | | | | | | | |
|---|---|---|---|---|---|---|---|
| **AMPK** | 40 | 100 V 2h | 5% milk 2h RT | 1:1000 5% BSA O/N | Cell signalling | Anti-rabbit (1:1000) milk 5% | Cell signalling |
| **CALPAIN 1 (μ-type)** | 40 | 100 V 2h | 5% milk 2h RT | 1:1000 5% milk O/N | Cell signalling | Anti-rabbit (1:1000) milk 5% | Cell signalling |
| **CALSEQUESTRIN** | 40 | 100 V 2h | 5% milk 2h RT | 1:1000 5% milk O/N | Abcam | Anti-rabbit (1:1000) milk 5% | Cell signalling |
| **CD31** | 40 | 100 V 2h | 5% milk 2h RT | 1:1000 5% milk O/N | Abcam | Anti-mouse (1:5000) milk 5% | DAKO |
| **CS** | 40 | 100 V 2h | 5% milk 2h RT | 1:2000 5% milk O/N | Abcam | Anti-rabbit (1:1000) milk 5% | Cell signalling |
| **DRP1** | 40 | 100 V 2h | 5% milk 2h RT | 1:1000 5% BSA O/N | Cell signalling | Anti-rabbit (1:1000) milk 5% | Cell signalling |
| **FIS1** | 40 | 100 V 2h | 8% milk 2h RT | 1:1000 5% milk O/N | Abcam | Anti-rabbit (1:1000) milk 5% | Cell signalling |
| **LDH** | 40 | 100 V 2h | 5% milk 2h RT | 1:1000 5% milk O/N | Abcam | Anti-rabbit (1:1000) milk 5% | Cell signalling |
| **MCT1** | 40 | 100 V 2h | 5% milk 2h RT | 1:1000 5% milk O/N | Sigma | Anti-mouse (1:5000) milk 5% | DAKO |
| **MCT4/SLC16A3** | 40 | 100 V 2h | 5% milk 2h RT | 1:1000 5% milk O/N | Sigma | Anti-rabbit (1:1000) milk 5% | Cell signalling |
| **MFN1** | 40 | 100 V 2h | 5% milk 2h RT | 1:1000 5% milk O/N | Abcam | Anti-mouse 1:5000 | DAKO |
| **MFN2** | 40 | 100 V 2h | 5% milk 2h RT | 1:1000 5% milk O/N | Abcam | Anti-rabbit (1:1000) milk 5% | Cell signalling |
| **OPA1** | 40 | 100 V 2h | 5% milk 2h RT | 1:3000 5% milk O/N | Abcam | Anti-mouse (1:5000) milk 5% | DAKO |
| **PGC1α** | 40 | 100 V 2h | 5% milk 2h RT | 1:1000 5% milk | Abcam | Anti-rabbit (1:1000) milk 5% | Cell signalling |
| **SERCA 1/ATP2A1** | 40 | 100 V 2h | 5% milk 2h RT | 1:1000 5%milk O/N | Cell signalling | Anti-rabbit (1:1000) milk 5% | Cell signalling |
| **SERCA 2 / ATP2A2** | 40 | 100 V 2h | 5% milk 2h RT | 1:1000 5%milk O/N | Cell signalling | Anti-rabbit (1:1000) milk 5% | Cell signalling |
| **SIRT1** | 40 | 100 V 2h | 5% milk 2h RT | 1:1000 5% BSA | Cell signalling | Anti-mouse (1:5000) milk 5% | DAKO |

***Table 2*** *List of primary and secondary antibodies used.*

*Myosin Heavy Chain Isoform* The Myosin Heavy Chain (MHC) isoform composition was assessed in the whole biopsy. Frozen portion of the biopsy was pulverized in a steel mortar with liquid nitrogen to obtain a powder that was immediately resuspended in a Laemmli solution (*Soriano et al., 2006*). The samples were incubated on ice for

20 min and finally spun at 18,000 g for 30 min. About 10 µg of proteins for each sample was loaded on 6% Sodium Dodecyl Sulphate polyacrylamide gels electrophoresis (SDS-PAGE) and electrophoresis was run overnight at 100 V; following Coomassie staining, three bands corresponding to MHC isoforms were separated and their densitometric analysis was performed to assess the relative proportion of isoforms MHC-I, MHC-IIA, MHC-IIX in the samples (*Brocca et al., 2017*). Image gels were acquired using a scanner (Epson Expression 1680 Pro) and densitometry was performed with a provided software (2202 Ultroscan Laser Densitometric Lkb). During analysis, protein bands were visualized as peaks and areas below peaks were measured and compared. In this way, it was possible to determine the percentage ratio between every isoform. Analysis of each sample was repeated three times and an average of three repeated measurements was calculated. The single value of MHC distribution obtained from each sample was averaged with the other values of subjects of the same group to assess the mean MHC isoform distribution.

### *Morphological and Histological Investigation*

Several transverse sections with a thickness of 10 µm each were obtained from muscle samples mounted in OCT (Tissue-Tek, Sakura Finetek Europe, Zoeterwoude, Netherlands). The working temperature, to ensure the consistency suitable for cutting the muscles, was set at 20-22°C. Sections were collected on the surface of a polarized glass slide, which guarantees the permanent adhesion.

#### *Capillarization and Cross-Sectional Area (CSA)*

Serial transverse muscle cryosections were fixed with methanol in ice for 15 min, washed 3 times (5 min each) in Phosphate Buffered Saline (PBS) buffer (NaCl 136 mM, KCl 2 mM, $Na_2HPO_4$ 6 mM, $KH_2PO_4$ 1mM) at room temperature and incubated in 0.01% Triton-100x in PBS for 30 min at room temperature. Cryosections were then incubated with blocking reagents (4% BSA in 0.01% Triton-100X in PBS + 5% Goat Serum) for 30 min at room temperature, raised with PBS (3 times for 5 min each) and probed with anti-CD-31 (1:50 dilution, Abcam) and anti-Dystrophin (1:500 dilution, Abcam) in 2% BSA in 0.01% Triton-100X in PBS + 5% Goat Serum) overnight at 4°C. After 3 washes (5 min each) in PBS, samples were incubated with Alexa-Fluor-594 anti-mouse (1:200 dilution, Abcam) and with Alexa-Fluor-488 (1:200 dilution, Abcam)

in 2% BSA in 0.01% Triton-100X in PBS + 5% Goat Serum for 60 min at room temperature. Fluorescence intensity was visualized with the fluorescence microscope (Leica Thunder Imager). The number of capillaries was counted under 10x objective. Capillary density was expressed as the number of capillaries per $mm^2$ muscle tissue. Different fields from each muscle were randomly selected, and the number of capillaries was counted. Fibre CSAs were measured with Image J analysis software (NIH, Bethesda, MD, USA) and expressed in $\mu m^2$.

**Epigenetics Analysis**

*Tissue Homogenization, DNA Isolation, and Bisulfite Conversion* Power analysis was conducted to detect a greater than 1.05 (5%) fold change in methylation based on our previous studies (*Seaborne et al., 2018a*), n = 3-4 in a within-subject design was determined as sufficient to detect statistically significant changes in methylation over the baseline, training, detraining, and retraining time points. Thereby, five subjects analyzed in the present study were sufficient to infer conclusions on changes in methylation. Tissue samples were homogenized for 45 s at 6,000 rpm × 3 (5 min on ice in between intervals) in lysis buffer (180 µl buffer ATL with 20 µl proteinase K) provided in the DNeasy spin column kit (Qiagen, United Kingdom) using a Roche Magnalyser instrument and homogenization tubes containing ceramic beads (Roche, United Kingdom). The DNA was then bisulfite converted using the EZ DNA Methylation Kit (Zymo Research, CA, United States) as per the manufacturer's instructions.

*Infinium Methylation EPIC Beadchip array* All DNA methylation experiments were performed in accordance with Illumina manufacturer instructions for the Infinium Methylation EPIC 850K BeadChip Array (Illumina, USA). Methods for the amplification, fragmentation, precipitation and resuspension of amplified DNA, hybridization to EPIC BeadChip, extension and staining of the bisulfite converted DNA (BCD) was conducted as in detailed in paper from Seaborne and colleagues (*Seaborne et al., 2018b*). EPIC BeadChips were imaged using the Illumina iScan System (Illumina, United States).

DNA methylation analysis, differentially methylated region (DMR) analysis and Self Organizing Map (SOM) profiling. Following DNA methylation quantification via Methylation EPIC BeadChip array, raw. IDAT files were processed using Partek

Genomics Suite V.7 (Partek Inc. Missouri, USA) and annotated using the MethylationEPIC_v-1-0_B4 manifest file. We first checked the average detection p-values for each sample across all probes. The mean detection p-value for all samples across all probes was 0.000295, and the highest for any given sample was only 0.000597, which is well below the recommended 0.01 in the Oshlack workflow (*Maksimovic et al., 2017*). We also produced density plots of the raw intensities/signals of the probes per sample. These demonstrated that all methylated and unmethylated signals were over 11.5 (mean median signal for methylated probes was 11.56 and for unmethylated probes 11.69), and the mean difference between the median methylation and median unmethylated signal was 0.13, well below the recommended difference of less than 0.5 (*Maksimovic et al., 2017*). Upon import of the data into Partek Genomics Suite we removed probes that spanned X and Y chromosomes from the analysis due to having both males and females in the study design, and although the average detection p-value for each sample was on average very low (no higher than 0.000597) we also excluded any individual probes with a detection p-value that was above 0.01 as recommended (*Maksimovic et al., 2017*). Out of a total of 865,859 probes removing those on the X & Y chromosome (19,627 probes) and with a detection p-value above 0.01 (4,264 probes) reduced the total probe number to 843,355 (note some X&Y probes also had detection p-values of above 0.01). We also filtered out probes located in known single-nucleotide polymorphisms (SNPs) and any known cross-reactive probes using previously defined SNP and cross-reactive probe lists identified in earlier EPIC BeadChip 850K validation studies (*Pidsley et al., 2016*). This resulted in a final list of 791,084 probes to be analyzed. Following this, background normalization was performed via functional normalization (with noob background correction) as previously described (*Maksimovic et al., 2012*). Following functional normalization, we also undertook quality control procedures via Principle Component Analysis (PCA), density plots by lines as well as box and whisker plots of the normalized data for all samples.

Any outlier samples were detected using Principle Component Analysis (PCA) and the normal distribution of β-values. Outliers were detected if they fell outside 2 standard deviations (SDs) of the ellipsoids and/or if they demonstrated different distribution patterns to the samples of the same condition. We confirmed that no samples demonstrated large variation [variation defined as any sample above 2 standard deviations (SDs) – depicted by ellipsoids in the PCA plots and/or demonstrating any differential distribution to other samples, depicted in the signal

frequency by lines plots]. Therefore, no outliers were detected in this sample set. Following normalization and quality control procedures, we undertook differentially methylated position (DMP) analysis by converting β-values to M-values [M-value = log2(β/ (1 – ββ)], as M-values show distributions that are more statistically valid for the differential analysis of methylation levels (*Du et al., 2010*). We undertook a one-way ANOVA for comparisons of baseline, training, detraining, and retraining muscle tissue. Any differentially methylated CpG position (DMP) with an unadjusted p-value of ≤ 0.01 was used as the statistical cut-off for the discovery of DMPs.

We then undertook CpG enrichment analysis on these differentially methylated CpG lists within gene ontology (GO) and KEGG pathways (*Kanehisa & Goto, 2000; Kanehisa et al., 2016, 2017*) using Partek Genomics Suite and Partek Pathway. Differentially methylated region (DMR) analysis, that identifies where several CpGs are consistently differentially methylated within a short chromosomal location/region, was undertaken using the Bioconductor package DMRcate (DOI: 10.18129/B9.bioc.DMRcate). Finally, in order to plot and visualize temporal changes in methylation across the timepoints we implemented Self Organizing Map (SOM) profiling of the change in mean methylation within each condition using Partek Genomics Suite.

### *Gene Expression Analysis*

*Tissue Homogenization, RNA Isolation, Primer Design, and rt-qRT-PCR* Skeletal muscle tissue muscle was homogenized in tubes containing ceramic beads (MagNA Lyser Green Beads, Roche, Germany) and 1 ml Tri-Reagent (Invitrogen, Loughborough, UK) for 45 s at 6,000 rpm×3 (and placed on ice for 5 min at the end of each 45-s homogenization) using a Roche Magnalyser instrument (Roche, Germany). RNA was extracted using standard Tri-Reagent procedure via chloroform/isopropanol extractions and 75% ethanol washing as per manufacturer's instructions. RNA pellets were resuspended in RNA storage solution (Ambion, Paisley, UK) and analyzed for (Nanodrop, ThermoFisher Scientific, Paisley, UK) an indication of quality (260/280 ratio of mean ± SD, 2.01 ± 0.10). Then a one-step RT-PCR reaction (reverse transcription and PCR) was performed using QuantiFast SYBR® Green RTPCR one-step assay kits on a Rotorgene 3000Q. Each reaction was setup as follows; 4.75 µl experimental sample (7.36 ng/µl totalling 35 ng per reaction), 0.075 µl of both forward and reverse primer of the gene of interest (100 µM

stock suspension), 0.1 µl of QuantiFast RT Mix (Qiagen, Manchester, UK) and 5 µl of QuantiFast SYBR Green RT-PCR Master Mix (Qiagen, Manchester, UK). Reverse transcription was initiated with a hold at 50 °C for 10 min (cDNA synthesis), followed by a 5 min hold at 95 °C (transcriptase inactivation and initial denaturation), before 40–50 PCR cycles of 95°C for 10 s (denaturation) followed by 60°C for 30 s (annealing and extension). Primer sequences for genes of interest and reference genes are included (Table 3). Gene expression analysis was performed on at least n = 11 per condition for all genes unless otherwise stated. All genes demonstrated no unintended targets via BLAST search and yielded a single peak after melt curve analysis conducted after the PCR step above. All relative gene expression was quantified using the comparative Ct (ΔΔCt) method. Individual participant's own baseline Ct values were used in ΔΔCt equation as the calibrator using RPL13a as the reference gene. The average Ct value for the reference gene was consistent across all participants and experimental conditions (18.57 ± 0.81, SD) with low variation of 4.36%.

| | Primer sequences | |
|---|---|---|
| **Target** | **Forward** | **Reverse** |
| ADAM19 (NM_033274.5) | 5'-TGAATGTGGCAGGAGACACC-3' | 5'-GGATCTTCCCACACTTCGCA-3' |
| FOXK2 (NM_004514.4) | 5'-GATGAGCAGACTCCCACACC-3' | 5'-ACCCTTGCTGTGCTCAAGTT-3' |
| GNGT2 (NM_031498.2) | 5'-CTTCAGCCAAGCCCAAGTCT-3' | 5'-GAGTGGGGAATGGGTTCACA-3' |
| INPP5A (NM_001321042.2) | 5'-AAAGGTCGCTGGCAAAGAGA-3' | 5'-CTTGACCATTTGCACTCGGG-3' |
| MTHFD1L (NM_001242767.2) | 5'-ACCAGAATTTGGCTGAGGAGG-3' | 5'-CGGCTTCACTGCTATCTGGA-3' |
| TMEM40 (NM_001284406.2) | 5'-GGCCTTGCTGGTGTGTTATC-3' | 5'-TCCGAAGTAGATGCCAACGG-3' |
| TPM2 (NM_001301226.2) | 5'-ATCAAACTGTTGGAGGAGAAGC-3' | 5'-CTTTGCCACAGACCTCTCG-3' |
| PDGFB (NM_002608.4) | 5'-AAGGACTGAACTCCATCGCC-3' | 5'-CAAAGAGCGACCCCATCAGT-3' |
| CAPN2 (NM_001146068.2) | 5'-CAGACACTCTCACCAGCGAT-3' | 5'-TTCGGGTAGTTCCTGCAACC-3' |
| MB21D2 (NM_178496.4) | 5'-TTACTTGGTGCCTGCTTGCT-3' | 5'-TTCTTCAACTGCACCTCGCT-3' |
| SLC16A3 (NM_001042422.3) | 5'-CATCACTGGCTTCTCCTACGC-3' | 5'-TCGCTGTAGCCGATCCCAAA-3' |
| SPPL2C (NM_175882.3) | 5'-AGGACACACTGGGCATTTCC-3' | 5'-GCAGTTCTTGAGAGTGGGCA-3' |

***Table 3*** *List of primers used for rt-PCR evaluations. RPL3a is the housekeeping used for normalization. Both primers (forward and reverse) are written 5'→ 3'.*

### *Statistical Analysis*

Results are reported as the mean ± SD. Outcome measures were assessed using one-way repeated measure ANOVA to determine significant overall main effects across baseline, training, detraining, and retraining time points. Once an overall effect was confirmed, statistical significance of the measured difference between groups

was assessed further by Newman-Keuls multiple comparisons test, and adjusted p values with the corresponding 95% confidence interval were reported.

For epigenetics analysis, methylome wide array data sets for baseline, training and retraining were analyzed for significant DMPs in Partek Genomics Suite (version 6.6). All gene ontology and KEGG signaling pathway analysis was performed in Partek Genomics Suite and Partek Pathway, on generated CpG lists of statistical significance ($p < 0.01$) across conditions (ANOVA) or contrasts between paired conditions. For follow up M-value difference in CpG DNA methylation analysis was performed via ANOVA in MiniTab Statistical Software (MiniTab Version 17.2.1). Statistical values were considered significant at the level of $p \leq 0.01$. All data represented as mean difference unless otherwise stated.

Follow-up rt-qRT-PCR gene expression was analyzed using both a repeated measures one-way ANOVA, to detect significant interactions across time for identified clusters of genes, and an ANOVA for follow-up of individual genes over time. For follow-up fold change in CpG DNA methylation analysis was performed via ANOVA in MiniTab Statistical Software (MiniTab Version 17.2.1). Statistical values were considered significant at the level of $p \leq 0.05$. All data represented as mean ± SEM unless otherwise stated.

Follow-up protein expression was analyzed using a repeated measures one-way ANOVA, to detect significant interactions across time for individual proteins. Statistical values were considered significant at the level of $p \leq 0.05$. All data is represented as mean ± SD unless otherwise stated.

# RESULTS AND DISCUSSION

### *Incremental exercise and skeletal muscle capillarization*

*Incremental exercise* Pulmonary gas exchange, ventilatory, cardiac, and metabolic variables attained at the limit of tolerance at baseline, training, detraining, and retraining are reported in Table 4. The initial training period resulted in a significant improvement in $VO_{2peak}$ both in relative and absolute values (+4.7 ± 2.6 ml·min$^{-1}$·kg$^{-1}$ and +0.304 ± 0.168 l·min$^{-1}$, respectively), corresponding to a 14% increase in both ($p<0.001$). After training, $W_{peak}$ increased significantly by 35 ± 14 W (+18% compared to baseline, $p < 0.001$). Values for $VO_{2peak}$ were significantly reduced after detraining compared to the training condition (-4.6 ± 2.5 ml·min$^{-1}$·kg$^{-1}$ and -0.274 ± 0.188 l·min$^{-1}$, both $p<0.001$), as were values for $W_{peak}$ (-30 ± 15 $W_{peak}$, $p < 0.001$). No significant differences were observed from the baseline (all $p > 0.99$). Retraining resulted in a significant increase in $VO_{2peak}$ (+3.8 ± 2.8 ml·min$^{-1}$·kg$^{-1}$) and $W_{peak}$ (24 ± 14 W) that was not different from the first training ($p = 0.97$ and $p = 0.45$, respectively).

| Time point | W | $\dot{V}O_2$ (ml·min$^{-1}$·kg$^{-1}$) | $\dot{V}O_2$ (l·min$^{-1}$) | $\dot{V}CO_2$ (l·min$^{-1}$) |
|---|---|---|---|---|
| Baseline | 199 ± 43 | 35.6 ± 7.1 | 2.324 ± 0.494 | 2,953 ± 0,639 |
| Training | 234 ± 47*# | 40.3 ± 7.0*# | 2.629 ± 0.527*# | 3.251 ± 0.747*# |
| Detraining | 204 ± 47 | 35.7 ± 7.0 | 2.354 ± 0.595 | 2.944 ± 0.757 |
| Retraining | 229 ± 47*# | 39.5 ± 7.0*# | 2.568 ± 0.548*# | 3.140 ± 0.713*§# |

| | $\dot{V}_E$ (l·min$^{-1}$) | RER | HR (beats·min$^{-1}$) | RPE |
|---|---|---|---|---|
| Baseline | 114,7 ± 26,1 | 1,27 ± 0.08 | 189 ± 9 | 18 ± 1 |
| Training | 123.0 ± 25.1*# | 1.24 ± 0.08 | 189 ± 7 | 18 ± 2 |
| Detraining | 108.7 ± 26.5 | 1.25 ± 0.05 | 186 ± 10 | 18 ± 2 |
| Retraining | 121.0 ± 29.4# | 1.22 ± 0.06 | 186 ± 9 | 19 ± 1 |

***TABLE 4*** *Peak values of pulmonary gas exchange, ventilatory, cardiac and metabolic variables attained at the limit of tolerance at baseline, training, detraining and retraining time points. W, peak power output, $VO_2$, oxygen uptake, $VCO_2$, carbon dioxide production, $V_E$, pulmonary ventilation, RER, respiratory exchange ratio; HR, heart rate; RPE, rating of perceived exertion. * $p < 0.05$ vs baseline; § $p < 0.05$ vs baseline, # $p < 0.05$ vs detraining. All Values are means ± SD. (n=16).*

*Skeletal muscle capillarization* The main adaptation processes in skeletal muscle that confer the oxidative metabolic phenotype to the aerobic exercise stimulus are structural and functional modifications of the mitochondria and the formation of new capillaries *(Geng et al., 2010)*. In this study capillary density (CD) and expression of the endothelial marker CD31 were measured to determine the vascular adaptations to different interventions.

CD levels increased after both training interventions and decreased to basal levels during detraining (Figure 10A). The protein expression levels of CD31 also significantly increased after both training interventions and remained stably high during detraining (Figure 10B).

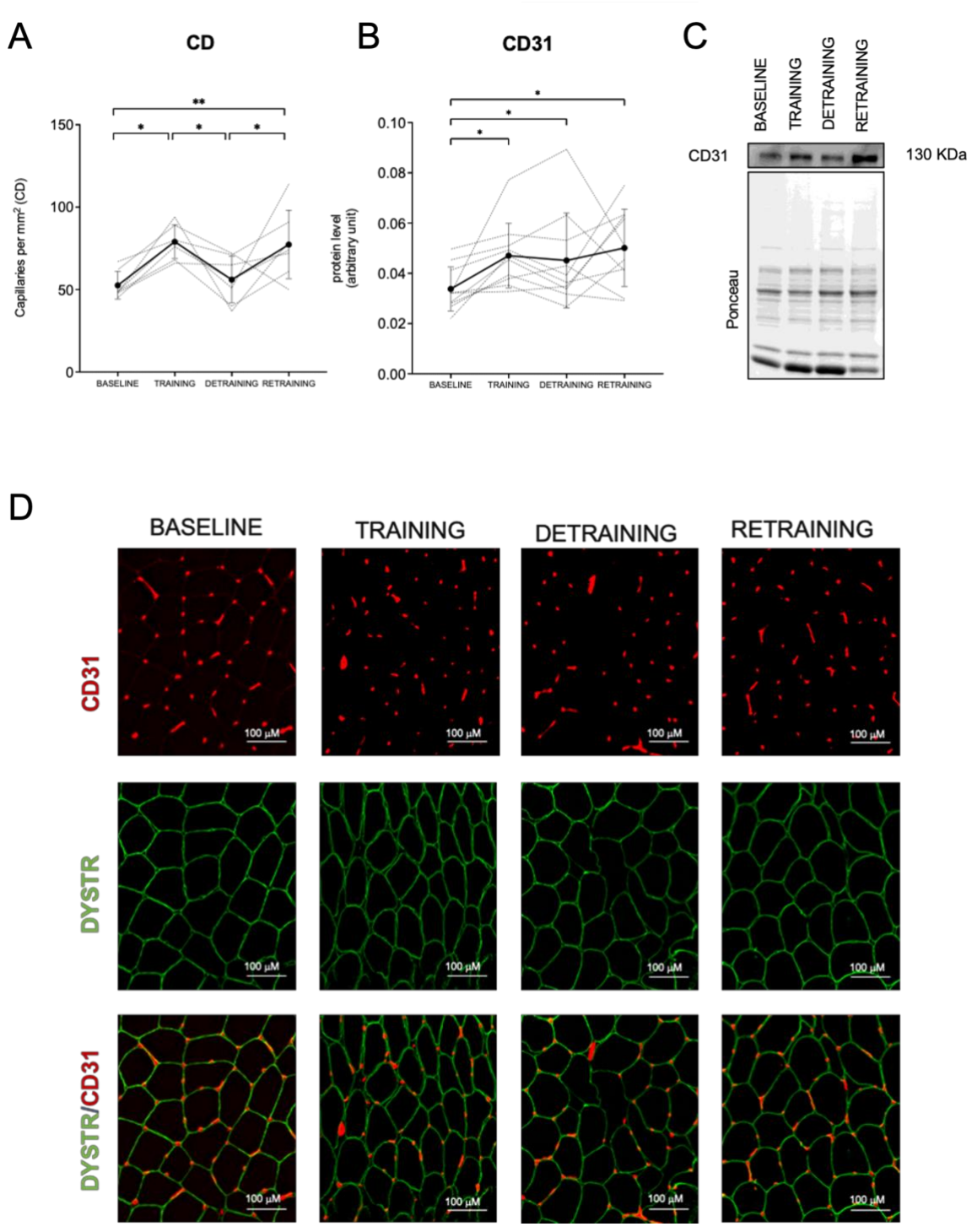


***Figure 10 A**) Capillary Density (CD) measured on transversal section of vastus lateralis muscle and **B**) protein expression changes in endothelial marker CD31 after a period of 8 weeks of high-intensity interval training (TRAINING), 12 weeks of exercise cessation (DETRAINING) and a subsequent secondary period of 8 weeks of high-intensity interval training (RETRAINING). **C**) Representative Western Blot image and corresponding Ponceau staining. Protein levels were normalized for Ponceau staining. **D**) Representative immunofluorescence images of transversal section of vastus lateralis muscle. Scale bar 100 µm. All Values are means ± SD. N = 10. *p < 0.0332, **p < 0.0021.*

Both interval training periods induced positive changes in functional indexes of endurance performance collected at the whole-body level. Peak power output and peak oxygen consumption were around 15% higher after the interventions, suggesting an improvement in endurance performance. (Table 4). However, no significant differences were observed in either peak power output or peak oxygen consumption between the training and the retraining period. This result is consistent with two previous studies on repeated interventions, where no differences were found in functional indexes of aerobic performance, comparing two repeated interventions of high-intensity interval training interspersed by a long-term period of training cessation *(Simoneau et al., 1987; Del Giudice et al., 2020).* These *in vivo* results suggest that physiological adaptations at the whole-body level do not benefit from repeated interventions.

The vascular response to interventions with exercise emerging from our data is consistent with the observed increase in capillarization as a response to the increased demand for oxygen during aerobic exercise. Several experimental studies have demonstrated the power of high-intensity interval exercise to induce capillarization *(Jensen et al., 2004; Scribbans et al., 2014; Tan et al., 2018)*. This process enhances the delivery of oxygen and nutrients to the working muscles, improving their efficiency and endurance. Overall, data on vascular remodelling paralleled the changes in peak oxygen consumption, suggesting a peripheral vascular contribution to endurance performance benefits. As for the *in vivo* functional indexes of endurance performance, also at the level of capillarization, no significant improvement was observed after the second training intervention again, suggesting the absence of a memory effect in response to aerobic training.

In this regard, it is important to note that continued training may not provide enough angiogenic stimulus to induce further capillary growth. Accordingly, in the study by *Jensen et al. (2004)*, after the initial 4 weeks of HIIT, an additional 3 weeks of training did not result in any further increases in capillarization, despite a progressive increase in training volume. Although the intensity of exercise training and the conditioned status of the muscle are a critical determinant of angiogenic potential *(Ross et al., 2023),* there is an idea that the tissue itself could become desensitised to the physiological signals *(Hellsten et al., 2015)*. Hoier and colleagues demonstrated that as training increases, the adaptive potential of skeletal muscle becomes attenuated *(Hoier et al., 2013)*. This was evidenced by the attenuation of molecular signaling responses involving the main Vascular Endothelial Growth Factor (VEGF) in skeletal

muscle, as well as the attenuated capillary growth *(Hoier et al 2013)*. After HIIT, VEGF protein levels were found to be lower *(Gliemann et al., 2015)*.

Our data also indicates that CD31 protein levels remain elevated during detraining, despite the capillary density returning to basal level. CD31 is a cell surface molecule found abundantly on endothelial cells as well as on leukocytes and platelets. It functions as a co-receptor with various mechanical, metabolic, and immune intracellular signaling pathways *(Caligiuri, 2019)*. Its expression may reflect other cellular processes that do not necessarily reflect changes in capillary density. Rather, the reduced capillary density is consistent with the documented reduction in VEGF during detraining *(Malek et al., 2010)*.

It is worth noting that high levels of CD31 were obtained during both training sessions and maintained during the detraining period, suggesting a potential muscle memory effect for this endothelial marker.

***Skeletal muscle phenotype and muscle fibres size***

Skeletal muscle fibres can adapt their structural and functional properties in response to new conditions, such as endurance exercise training. This adaptation can cause changes in muscle fibre composition, resulting in functional (slow-fast transitions) and metabolic (glycolytic-oxidative transitions) remodelling. Furthermore, the size of the fibres may also change in response to specific training programs. To investigate the effects of training and detraining interventions on the shift and size of muscle fibres, we analyzed the composition of MHC isoforms using electrophoretic analysis, and the cross-sectional area (CSA) of single fibres using histological analysis.

Figure 11A shows that the percentage of MHCI, MHCIIA and MHCIIX were not affected by the examined conditions, suggesting no shift in fibre-type in response to the two high-intensity interval training interventions and detraining. These data are consistent with previous studies, reporting HIIT dot change skeletal muscle fibre-type composition in terms of myosin heavy chain isoforms in human *(Hostrup et al., 2022; Kohn et al., 2010)*.

No significant effect of training, detraining, and retraining on single fibre size was found regarding fibre size (Figure 11C). Given that fibre size remained constant throughout the interventions, it is reasonable to assume that there was no change in myonuclei density under the examined conditions. These findings are consistent with the results reported by Joanisse and his colleagues *(Joanisse et al., 2015)*, where no

effects of 6 weeks of low-volume HIIT were observed on either fibre size or myonuclear content.

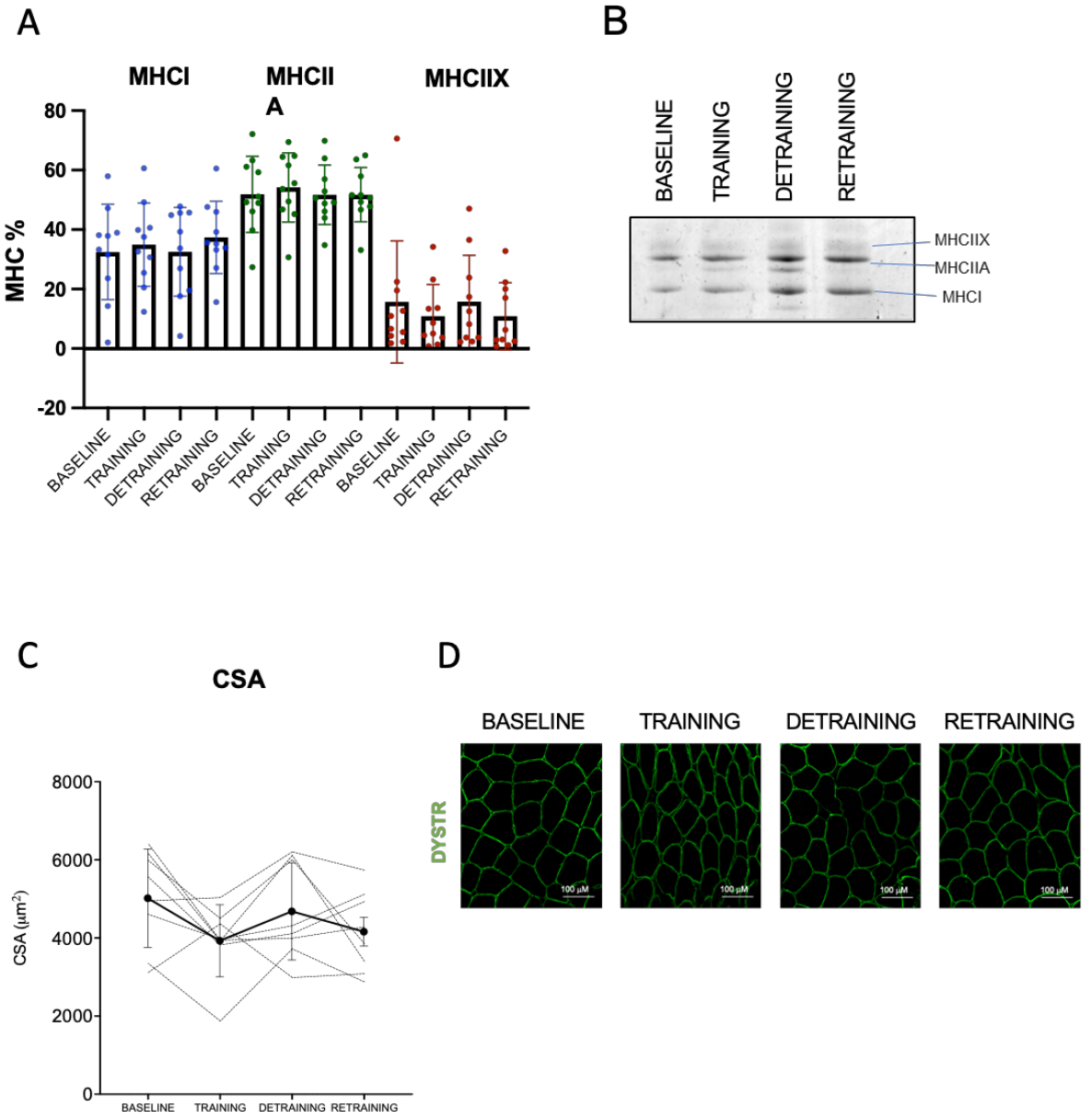


***Figure 11 A**) Composition of myosin heavy chain (MHC) isoforms determined with SDS-PAGE and **B**) relative representative image **C**) Cross-sectional area (CSA) of single muscle fibres measured on immunofluorescence images of transversal section of vastus lateralis muscle and **D**) relative representative image. Scale bar 100 µm. All measurements were carried out after a period of 8 weeks of high-intensity interval training (TRAINING), 12 weeks of exercise cessation (DETRAINING) and a subsequent secondary period of 8 weeks of high-intensity interval training (RETRAINING). All Values are means ± SD. N = 10.*

### *Mitochondrial Adaptations*

Although no significant insights into muscle memory have been found at the whole-body level, protein expression level of the endothelial marker CD31 suggested a potential muscle memory profile. Therefore, it is not excluded, that a more in-depth investigation at the skeletal muscle level may detect a cellular or molecular muscle memory. Thus, we examined the response of crucial biomarkers of mitochondrial biogenesis, dynamics, and mitochondrial respiration. Previous studies have demonstrated that aerobic exercise triggers stress signals, that enhance the expression of genes related to these processes.

*Mitochondrial content and biogenesis factors* Mitochondrial density/content was assessed by measuring the levels of CS protein, an enzyme localized in the mitochondrial matrix. The results showed a significant main effect for time ($p < 0.0332$) after repeated measures of one-way ANOVA analysis. After the initial training, there was a tendency towards an increase of CS content. Furthermore, CS content significantly increased in response to retraining compared to both detraining and baseline (Figure 12A). These findings suggest a gradual increase in mitochondrial content, which only becomes significant after the second training.

Key factors involved in mitochondrial biogenesis were evaluated as a possible cause of the increased mitochondrial mass. PGC-1α is the most important regulatory factor involved in mitochondrial biogenesis and general energy metabolism. After repeated measures one-way ANOVA analysis, PGC-1α exhibited a significant main effect for time ($p < 0.0021$). Its protein level exhibited a trend to increase after training and significantly increased after retraining (Figure 12B). Notably, changes in PGC-1α were observed to parallel changes in CS content, indicating that both proteins undergo similar modulation in response to repeated training, and detraining interventions.

Furthermore, the levels of SIRT1 and AMPK activation were also determined, as these two metabolic sensors can directly affect PGC-1α activity through deacetylation and phosphorylation, respectively. The data showed that repeated high-intensity exercise had no effect on SIRT1 protein levels (Figure 12C). Additionally, there were no significant changes in AMPK activation, as indicated by the analysis of the active (phosphorylated) and total form of AMPK (Figure 12D-E).

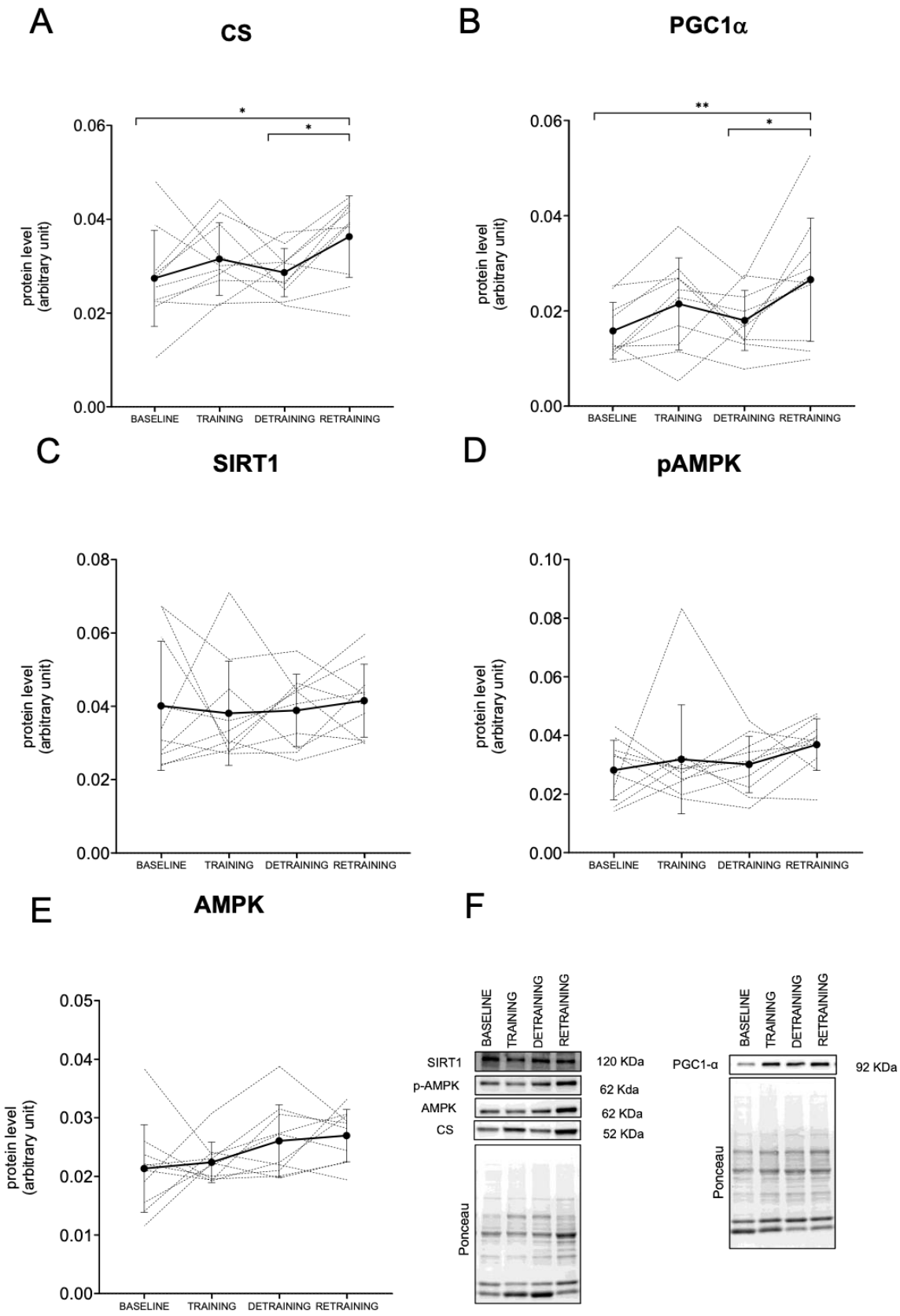


***Figure 12*** *Relative protein expression changes of mitochondrial biomarkers after a period of 8 weeks of high-intensity interval training (TRAINING), 12 weeks of exercise cessation (DETRAINING) and a subsequent secondary period of 8 weeks of high-intensity interval training (RETRAINING.* ***A)*** *Citrate synthase (CS),* ***B)*** *PGC1α* ***C)*** *SIRT1* ***D)*** *AMPK* ***E)*** *p-AMPK* ***F****) Representative Western Blot image and corresponding Ponceau staining. Protein levels were normalized for Ponceau staining. All Values are means ± SD. N = 10. *p < 0.0332, **p < 0.0021.*

*Mitochondrial dynamic factors* The morphology of the mitochondrial network, proteins related to dynamics, and energy metabolism are highly correlated. Changes in the cellular energy state during exercise may also occur through the dynamics of the mitochondrial network. Although mitochondrial remodelling is a crucial regulatory process in maintaining mitochondrial function, our understanding of how repeated exercise regulates mitochondrial dynamics is limited. It is not clear how repeated interventions of high-intensity aerobic exercise interspersed with a long period of detraining may affect this process. Mitochondrial morphology is adapted to bioenergetics through the regulation of fusion-fission events. Previous research has demonstrated that PGC-1α/ERRα recognizes the MFN2 promoter, inducing its expression in cell cultures *(Cartoni R., et al., 2005)*. This highlights how PGC-1α not only regulates mitochondrial biogenesis but also mediates mitochondrial architecture, in response to aerobic exercise in humans *(Cartoni R., et al., 2005)*. The present study analyzed mitochondrial dynamics by examining the expression levels of pro-fission and pro-fusion proteins. The expression of protein markers involved in fission/fusion events showed a significant main effect of time, as shown by repeated measures of one-way ANOVA analysis for MFN1, MFN2 ($p < 0.0021$), DRP1 ($p < 0.0332$), and OPA1 ($p < 0.0001$).

Overall, the data on mitochondrial dynamics indicated a training-induced pro-fusion effect. Specifically, among the interventions performed, no significant changes were observed in the expression of FIS1 fission marker, while DRP1 increased its expression after retraining in comparison to baseline. Significant increases in protein markers MFN2 and OPA1 were observed following each training period. Notably, protein levels for MFN2 remained high even during detraining, while OPA1 returned to expression levels similar to baseline. Additionally, MFN1 protein significantly increased during retraining compared to the initial training (Figure 13).

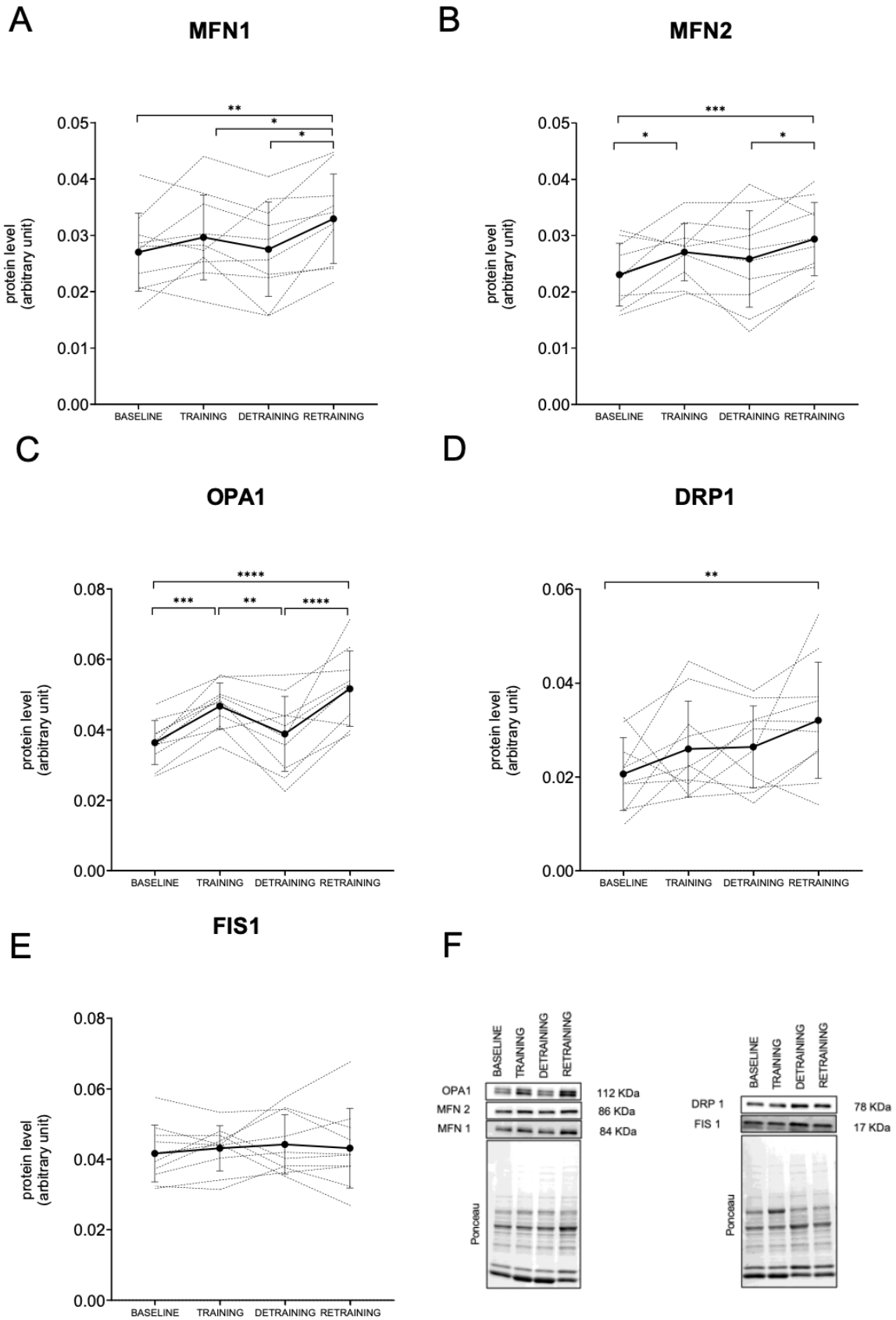


***Figure 13*** *Relative protein expression changes of mitochondria dynamics biomarkers after a period of 8 weeks of high-intensity interval training (TRAINING), 12 weeks of exercise cessation (DETRAINING) and a subsequent secondary period of 8 weeks of high-intensity interval training (RETRAINING).* ***A)*** *pro-fusion mitofusin 1 (MFN1).* ***B)*** *pro-fusion mitofusin 2 (MFN2)* ***C)*** *pro-fusion OPA1.* ***D)*** *pro-fission DRP1.* ***E)*** *pro-fission FIS1.* ***F****) Representative Western Blot image and corresponding Ponceau staining. Protein levels were normalized for Ponceau staining. All Values are means ± SD. N = 10. *p < 0.0332, **p < 0.0021, ***p < 0.0002, ****p < 0.0001.*

*Mitochondrial respiration* The study investigated the effect of high-intensity interval training interventions on mitochondrial function. Mitochondrial electron chain (ETC) efficiency was evaluated using the Oroboros O2k technique, and the SUIT (substrate-uncoupler-inhibitor titration) protocol was used to target complexes I and II. The results are presented in figure 14. The leak phase, which indicates proton dissipation not associated with oxidative phosphorylation, was only evaluated in complex I. Glutamate and Malate substrates were added to stimulate the reaction. There was no change in proton leakage after the two training interventions, indicating that protons were not further dissipated during mitochondrial respiration under the training stimulus in comparison to baseline. The system was able to prevent the loss of spare protons, which play a crucial role in the efficiency of ETC mechanism. In contrast, a significant decrease was observed after detraining. We assessed the capacity for oxidative phosphorylation by analyzing OXPHOS, following submaximal titrations at ADP saturation (Figure 14B-C). The study found that the system did not undergo any intrinsic changes under the tested conditions.

The electron transport system (ETS) was evaluated for its ability to transport electrons without ATP production, which is characterized by all-electron flows promoted by the ETC. No differences in the maximum efficiency of the ETS were observed among interventions. (Figure 14D-E).

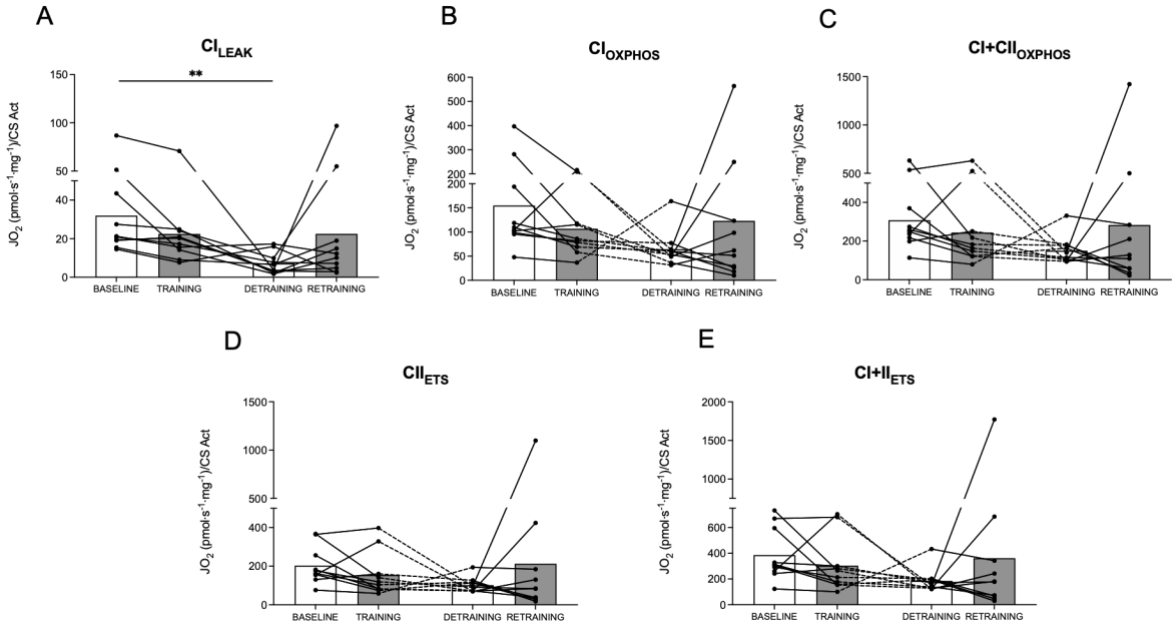


***Figure 14*** *Mitochondrial respiration measured with high-resolution respirometry in permeabilized fibres obtained from biopsy on vastus lateralis muscle at baseline, training, detraining and retraining time points.* ***A****) Mass-specific mitochondrial 0₂ flux values of leak respiration through CI,* ***B****) maximum coupled mitochondrial respiration through CI,* ***C****) maximum coupled mitochondrial respiration through CI+CII,* ***D****) maximum uncoupled mitochondrial respiration through CII,* ***E****) maximum uncoupled mitochondrial respiration through CI+CII Mass-specific mitochondrial. O₂ flux values are expressed per mg of muscle dry weight and normalized on citrate synthase activity. All values are means ± SD. ** p < 0.0021. N = 10.*

The increase in PGC-1α and CS content, a validated marker of mitochondrial volume in human muscle *(Larsen et al., 2012)*, suggest an improvement in mitochondrial content and biogenesis after the second exposure to the training protocol. These adaptations are consistent with the training effects of HIIT observed in humans. It has in fact been demonstrated that there is an increase in both citrate synthase and mitochondrial biogenesis in *vastus lateralis* biopsies of subjects undergoing 5 weeks of HIIT *(Hostrup et al., 2022)*. These effects were also confirmed by structural analysis of mitochondria, which showed an increase in mitochondrial volume, number, and perimeter after 12 weeks of HIIT *(Ruegsegger et al., 2023)*.

Although several studies suggest that aerobic exercise induces mitochondrial biogenesis by activating the AMPK/PGC-1α axis, no AMPK activation was detected in this study. The regulation of AMPK activity in skeletal muscle can vary depending on factors such as training state and exercise intensity. There is evidence that the activation of AMPK in skeletal muscle by acute exercise is reduced after a period of training *(Nielsen et al., 1985; McConnell et al., 2005)*. On this basis, the unchanged levels of AMPK activation found in this study, are in line with the concept that with regular endurance training, skeletal muscles may undergo chronic adaptations that reduce AMPK signaling.

Regarding the modulation of PGC-1α by the deacetylase SIRT1, the stable SIRT1 levels in response to exercise interventions are consistent with a recent study, showing that although HIIT changes acetylome in skeletal muscle, SIRT1 abundance remains unchanged in response to HIIT *(Hostrup et al., 2022)*.

Based on these results, we speculated that the regulation of enhanced PGC-1α content after retraining is due to transcriptional mechanisms rather than post-translational mechanisms, as it is not accompanied by SIRT1 induction and AMPK activation. However, it cannot be ruled out that there may a post-translational effect by the Calcium/calmodulin serine/threonine kinase (CaMK). Training induces responses through the Calcium/calmodulin serine/threonine kinase (CaMK) signaling pathway, which interacts with downstream transcriptional regulators following increases in intramuscular calcium associated with muscle contraction *(Fernandez-Marcos et al., 2011; Booth et al., 2015)*. This pathway converges on the transcription factor co-activator PGC-1α *(Fernandez-Marcos et al., 2011)*, similar to AMPK.

Additionally, factors related to aerobic metabolism may also change in response to fibre-type transition process. It is widely recognised that slow-twitch fibres, which rely more on aerobic metabolism, typically exhibit higher levels of citrate synthase and

PGC-1α in comparison to fast-twitch fibres *(Lloyd et al., 2023; Zhang et al., 2017)*. The observed increase in PGC-1α and CS in response to the different interventions does not appear to be dependent on a transition of fibre types, as suggested by the unchanged MHC isoforms composition. However, this finding also supports the hypothesis of a possible transcriptional effect.

Data on mitochondrial fission and fusion markers confirm, and extend what is known from the few studies, about the effect of HIIT training on mitochondrial dynamics. The positive modulation of mitofusions proteins, and OPA1, together with the unchanged fission proteins FIS1, and the slight changes in DRP1 (retraining vs baseline), are suggestive of a shift in balance from fission to fusion. A similar effect was reported by Ruegsegger and his colleagues *(Ruegsegger et al., 2023),* in which HIIT was found to be associated with increased protein level of OPA1 and increased ratio of OPA1/FIS1 correlated with a larger, more fused mitochondrial tubular network evaluated by electron microscopy in skeletal muscle. Interestingly, the same authors found a correlation between pro-fusion proteins and mitochondrial respiration in response to HIIT. Other authors have also observed that HIIT leads to an increase in mitochondrial respiration *(Granada et al., 2018)*. Surprisingly, our data on mitochondrial respiration did not show any improvement in mitochondrial function in response to training interventions. Therefore, the response observed for the present study was unexpected. In this proposal, it is worth noting that an increase in mitochondrial content does not always correspond to an increase in mitochondrial respiration, as found in our case *(Montero et al., 2015)*. Additionally, without modulation of AMPK, there is no necessarily expected effect on mitochondrial respiration. Lantier and his colleagues *(Lantier et al., 2014)*, using skeletal muscle-specific AMPKα1α2 double-knockout mice, showed that AMPK levels impact mitochondrial oxidative capacity independently of mitochondrial content.

Taken together, the collected results provide further support for the hypothesis of the presence of possible memory regulatory mechanisms, triggered by repeated aerobic training. This is mainly evident from the following observations: a) some of the analysed factors showed a protein expression profile with the highest levels of expression observed after exposure to the second exercise training. These factors include CD31, citrate synthase, PGC-1α and mitofusin1. b) It is noteworthy that the observed trend in PGC-1α and citrate synthase expression levels is not affected by a transition in fibre types. c) Additionally, the observed trend in PGC-1α expression levels does not seem to be determined by a post-translational mechanism. d) CSA of

individual fibres remained constant throughout the interventions, speculating that there was no change in myonuclei density.

Added to this is the proven effectiveness of acute high-intensity exercise leading to DNA hypomethylation, and subsequent increase in gene expression in metabolic and oxidative biomarkers compared to low-intensity training at the target gene level (*Barrès et al., 2012*), and across the methylome (*Masaar et al., 2021*), which leads to the suggestion that the same pattern may occur in response to chronic interventions. In this scenario, it is reasonable to assume that determining protein profiles in response to exercise, could be a transcriptional mechanism mediated by epigenetic modifications. Therefore, epigenetic analysis was performed on skeletal muscle tissue.

### *Genome-wide DNA methylation analysis*

*Differentially methylated CpG positions* The frequency of statistically differentially methylated CpG positions (DMPs) in each condition was analyzed (Figure 15), and a list of 35.855 DMPs was identified. Following initial interval training 21.605 CpG sites were significantly differentially methylated compared to baseline with a larger number being hypomethylated (14.516) compared to hypermethylated (7.089). After detraining, the total number of DMPs decreased (3.854), anyway most of them were hypomethylated (3.349), whereas hypermethylated DNA sites nearly reverted to baseline (505). Following retraining, we observed another increase in the number of DMPs (10.396) with most CpGs hypomethylated (9.644), compared to hypermethylated DNA sites that remained similar to detraining (752) (Figure 15A). Although increment in hypomethylated CpGs during retraining was smaller compared to the initial training period, when expressed as percentage of total differentially methylated sites, we observed a shift towards a hypomethylated profile across training (67%), detraining (87%), and retraining (93%) (Figure 15B). This was due to another large increase in hypomethylation after retraining, but also a much smaller

number of DMPs that were hypermethylated (752) during retraining compared to the earlier training period (7.089).

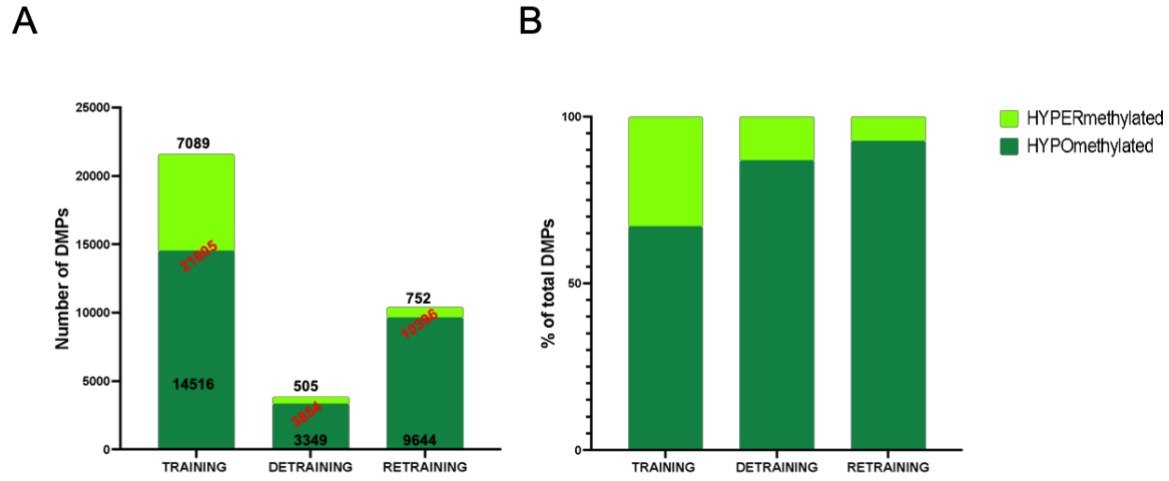


***Figure 15 A**) Total number of DMPs hypo – (dark green) and hyper-methylated (light green) following training, detraining, and retraining conditions compared to baseline (n = 5). **B**) Hypo (dark green) and hypermethylated (light green) DMPs as a percentage of the total number of DMPs (n = 5).*

*Self-organizing map (SOM) profiling* In order to investigate whether there were any similarly altered DMPs between training, detraining, and retraining, we overlapped DMP lists from analysis described above to detect CpG sites differentially methylated in the three conditions versus baseline. 5334 DMPs were identified overlapping across training, detraining, and retraining. Among these, 806 were common to all conditions (Figure 16A). Changes in genome-wide DNA methylation related to the 5334 DMPs commonly identified across experimental conditions were analyzed, and self-organizing map (SOM) profiling (or clustering) highlighted four temporal trend profiles of the DMPs (Figure 16B). The first temporal profile (named Signature 1) included 1190 DMPs that were hypomethylated after the initial training period. Importantly, hypomethylation was then retained as hypomethylated even during detraining, and this hypomethylation was then maintained into the later retraining period. The second temporal profile (Signature 2) included 2000 DMPs, and included DMPs that displayed hypomethylation after initial training, with a small reduction in hypomethylation as a result of detraining, although maintaining slightly hypomethylated status. As with Signature 1, retraining led to further hypomethylation during retraining at similar or at an enhanced level compared with the earlier training period. The third profile (Signature 3) included 1675 DMPs and, as previous two, displayed hypomethylation with first bout of training. Differently, this cluster became hypermethylated with detraining but reverted to hypomethylation state after retraining. The final profile (Signature 4) included the fewest 469 DMPs that were

hypermethylated after the initial training period. Then, these sites demonstrated a small reduction in hypermethylation with detraining and reverted to a more hypermethylated profile after later retraining.

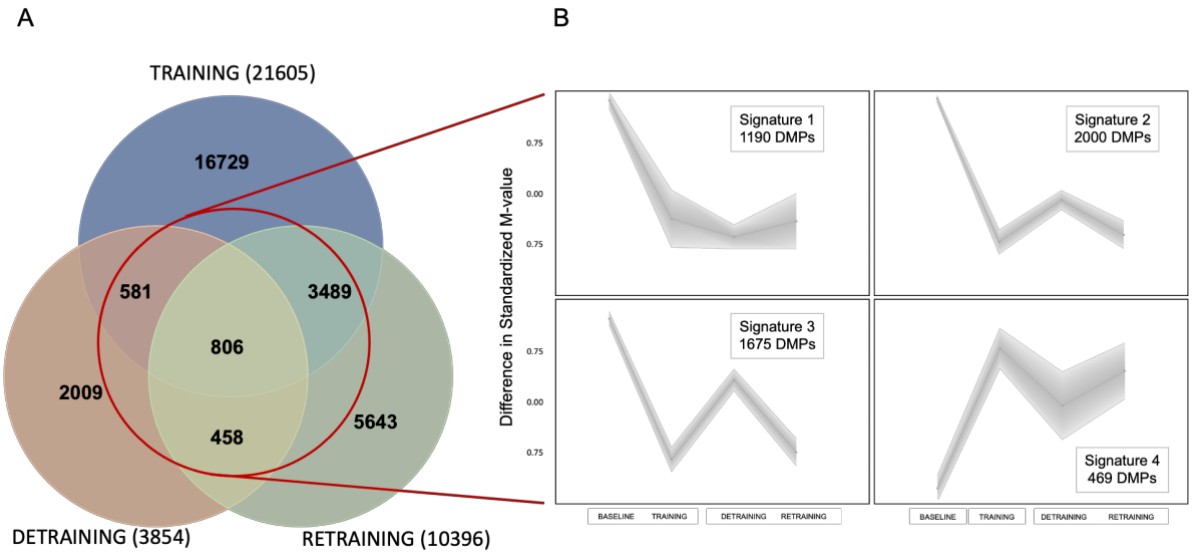


***Figure 16 A**) Venn diagram analysis of the statistically differentially regulated CpG sites following training, detraining, and retraining compared to baseline. Ellipsis reports number of common overlapping significant DMPs across each condition (n = 5). **B**) SOM profiling depicting the temporal regulation of DMPs over the time-course of baseline, training, detraining, and retraining.*

*Identification of epigenetic memory genes profiles and their expression* To assess whether the changes in DNA methylation across all conditions affected specific genes more frequently, we undertook differentially methylated region (DMR) analysis of the DMPs in signatures 1-4 identified above (Figure 17). DMR analysis identified several regions located in or close to annotated genes with enriched (multiple CpGs in short chromosomal regions) differential methylation in at least 2 pairwise comparisons. In signature 1 there were 6 DMRs discovered for genes: ADAM19, FOXK2, GNGT2, INPP5a, MTHFD1L, TMEM40. Five DMRs were identified with the Signature 2 profile: CAPN2, PDGFB, MB21D2, SLC16A3, and SPPL2C. For Signature 3, no genes with DMRs from cross-reference were detected, while Signature 4 characterized only one gene TPM2.

As shown in Figure 17A, expression of genes included in Signature 1 displayed a significant main effect for time ($p < 0.01$) after repeated measures one-way ANOVA analysis. After training, this cluster displayed increased gene expression that further increased during detraining, resulting in statistical significance compared to baseline alone. Gene expression was then retained upon retraining compared to baseline (Figure 17A). Signature 2 gene expression cluster displayed a significant effect of

time ($p < 0.01$) after repeated measures one-way ANOVA analysis . Upon first period of training, gene expression of this cluster significantly increased. Again, even during exercise cessation and detraining, gene expression displayed further increases that then was maintained during retraining compared to baseline alone (Figure 17B).

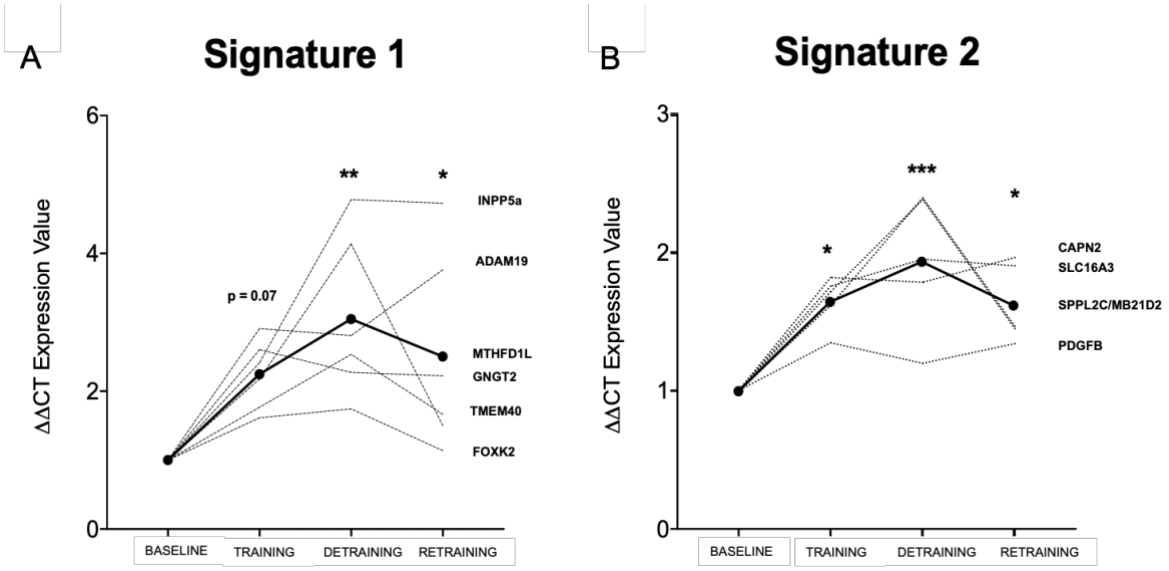


***Figure 17*** *Gene expression analysis of **A**) gene clusters outlined by Signature 1 (ADAM19, FOXK2, GNGT2, INPP5a, MTHFD1L, TMEM40). (N = 15) **B**) gene clusters outlined by Signature 2 (CAPN2, PDGFB, MB21D2, SLC16A3, SPPL2C) (N = 15). All significance refers to the comparison with the baseline * $p < 0.05$, ** $p < 0.01$, *** $p < 0.001$.*

Interestingly, in our clusters of genes identified above, the temporal gene expression pattern was inversely associated to the related DMP and DMR methylation. Closer fold-change analysis of CpG DNA methylation of these gene clusters identified a distinct inverse relationship with methylation and gene expression of 6 out of 11 of the targets (ADAM19, INPP5a, MTHFD1L, PDGFB, CAPN2, SLC16A3, (Figure 18). Where upon training, hypomethylation of these genes was associated with increased gene expression. Importantly, this hypomethylated profile was retained during detraining, and gene expression was retained as elevated (ADAM19, MTHFD1L, CAPN2, SLC16A3). Then these genes continued to possess retained hypomethylated into the retraining conditions where gene expression also remained elevated. Collectively, we report that a sustained hypomethylated state in 6 out of 11 of the genes in these clusters corresponds to an increased transcript expression after training, that is maintained into detraining (Figure 18).

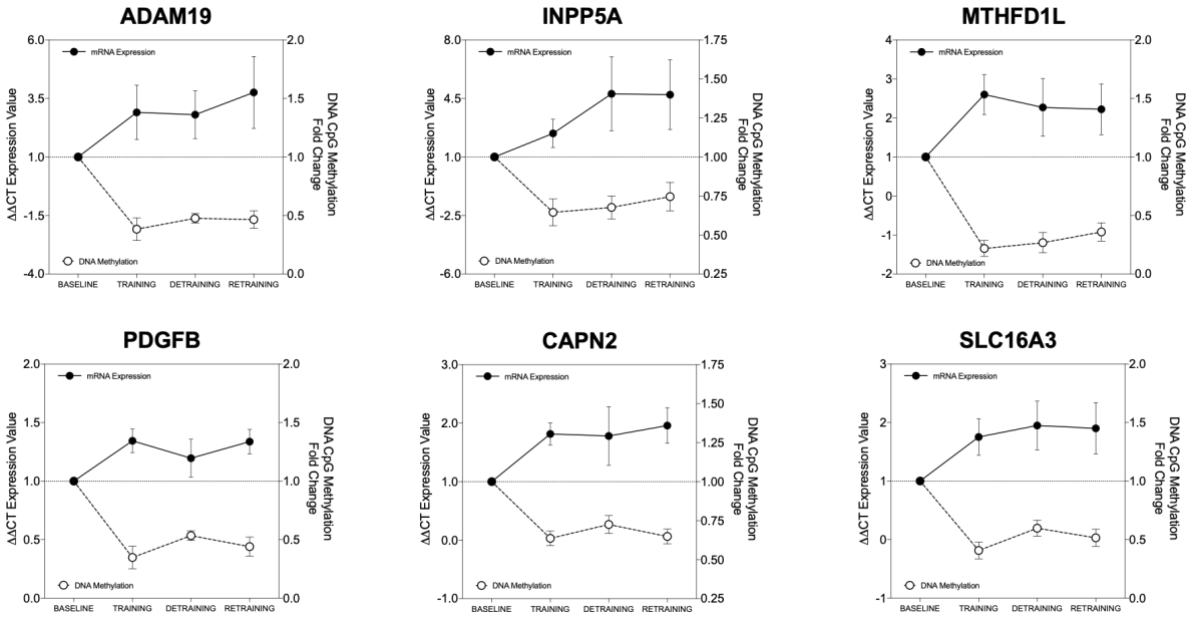


***Figure 18*** *Relationship between fold changes in mRNA expression (solid black line and black dots; left y-axis) and difference change in CpG DNA methylation within each DMR (dashed black line and white dots; right y-axis) across experimental conditions for identified genes: ADAM19, INPP5a, MTHFD1L, PDGFB, CAPN2, SLC16A3. All data is presented as mean ± SEM (N = 15).*

<u>*Epigenetically regulated genes and protein content*</u> Since retention of transcript expression was observed in genes involving mostly lactate transport (SLC16A3) and calcium signaling (CAPN2), to assess whether these main pathways were affected by retention or enhanced protein expression across conditions, lactate transport and calcium signaling biomarkers were investigated.

Measurements of protein expression changes in lactate transport biomarkers are reported in Figure 19. MCT1 displayed a significant main effect for time ($p < 0.05$) after repeated measures one-way ANOVA analysis. After the retraining, this protein displayed increased expression compared to baseline alone, and even a tendency to a greater expression than after initial training (Figure 19A). No changes are evident in the MCT4 and LDH patterns across repeated training interventions (Figure 19B-C).

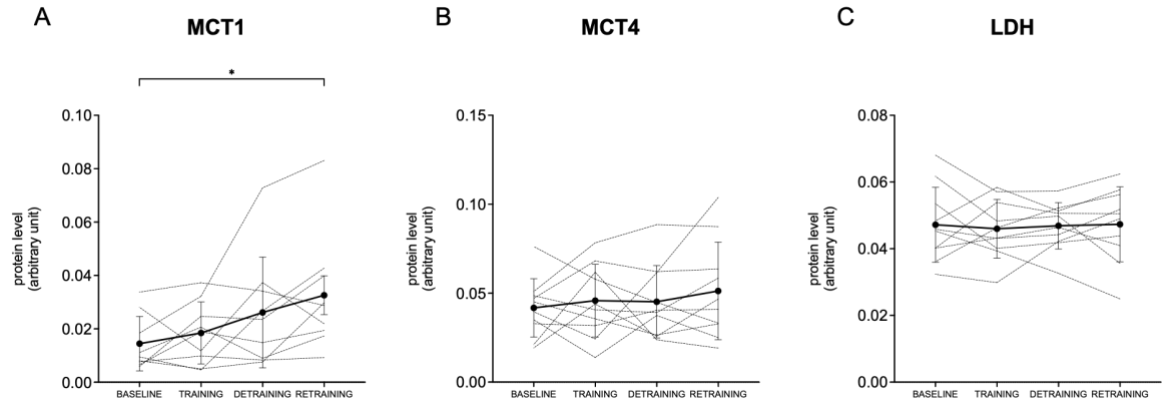


***Figure 19*** *Relative protein expression changes of lactate transport biomarkers after a period of 8 weeks of high-intensity interval training (training), 12 weeks of exercise cessation (detraining) and a subsequent secondary period of 8 weeks of high-intensity interval training (retraining).* ***A****) Monocarboxylate Transporter 1 (MCT1)* ***B****)*

*Monocarboxylate Transporter 4 (MCT4) and **C**) Lactate dehydrogenase (LDH). All Values are means ± SD. N = 10. *p < 0.0332.*

Measurements of protein expression changes in calcium signaling biomarkers are reported in Figure 20. No significant changes were observed in the protein levels of SERCA2, CLSQ1&2, CAPN1$_{(78KDa)}$, CAPN1$_{(80KDa)}$ and CAPN1(78KDa): CAPN1$_{(80KDa)}$ ratio, among the different interventions.

Repeated measures one-way ANOVA analysis reported for SERCA1 a significant effect of time ($p < 0.01$). Upon the first period of training, expression of this protein significantly decreased compared to baseline alone. During detraining, protein expression reverted to values not different from baseline condition. Protein expression then decreased again upon retraining compared to baseline ($p < 0.05$) (Figure 20A).

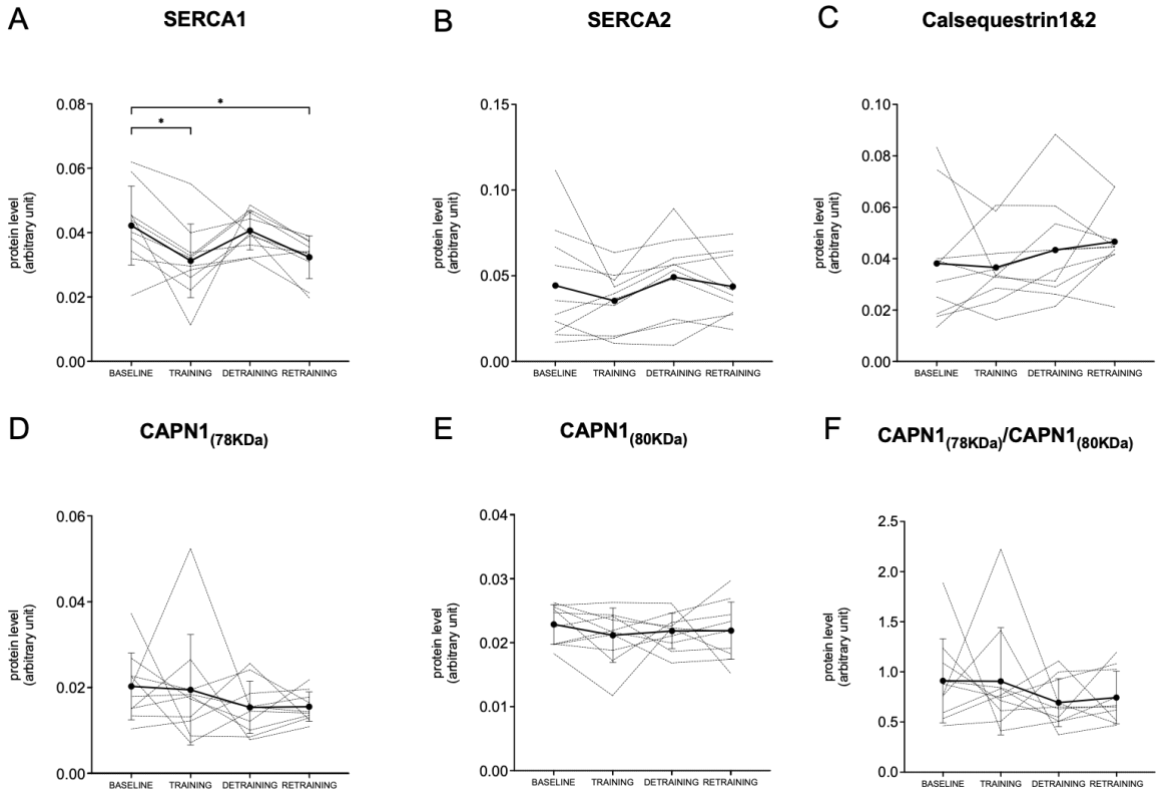


***Figure 20** Relative protein expression changes of calcium signaling biomarkers after a period of 8 weeks of high-intensity interval training (training), 12 weeks of exercise cessation (detraining) and a subsequent secondary period of 8 weeks of high-intensity interval training (retraining): A) sarcoplasmic/endoplasmic reticulum calcium ATPase 1 (SERCA1), **B**) sarcoplasmic/endoplasmic reticulum calcium ATPase 2 (SERCA2), C) calsequestrin 1&2 (CASQ1&2); **D**) calpain 1 (CAPN1$_{(78KDa)}$); **E**) calpain 1 (CAPN1$_{(80KDa)}$) and **F**) CAPN1$_{(78KDa)}$: CAPN1$_{(80KDa)}$ ratio. Protein levels were normalized for Ponceau staining. All Values are means ± SD. N = 10. *p < 0.0332*

Epigenetics analysis on skeletal muscle tissue revealed interesting findings, demonstrating extensive modifications via DNA methylation across training, detraining, and retraining periods. The total number of differentially methylated CpG sites increased during both training periods, with a less exaggerated response after

retraining, and reduced after detraining (Figure 15A). Simultaneously, the change also affected the state of methylation modification, which appears to gradually shift towards a more hypomethylated profile throughout conditions (Figure 15B). As previously described *(Nitert et al., 2012; Rowlands et al., 2014; Stephens et al., 2018*), endurance training induced greater hypomethylation at CpG sites compared to number of hypermethylated positions, suggesting greater ability to switch on expression for some of the same genes. Consistently, cessation of training reduced the total number of differentially methylated positions, however, although reduced, the number of hypomethylated DMPs remained higher showing an absence of reversion to the baseline level. Thus, a retention of hypomethylation from the training into the detraining period when exercise training was completely ceased. In contrast, during detraining hypermethylated CpG sites from the earlier training were nearly reversed back towards baseline levels. Interestingly, during retraining, although smaller in magnitude compared to the initial training, hypomethylation increased again, but surprisingly number of hypermethylated DMPs was maintained at levels similar to the previous condition after detraining, indicating that subsequent repeated interval retraining stimulus elicited a larger number of hypomethylated sites after retraining when compared to the number of those hypermethylated, similar to the epigenome modification found in response to chronic hypertrophic stimuli (*Seaborne et al., 2018b*).

More specific DNA methylation analysis identified two signatures of temporal DNA methylation patterns, that provide initial evidence of an epigenetic memory (Figure 17). The hypomethylation response observed in Signature 1 and 2 during the initial training period persisted even after detraining, despite the cessation of exercise. Furthermore, this hypomethylation status was maintained throughout the retraining phase. These temporal trends, marked by the retention of hypomethylation during the long-term interruption phase from the training stimulus, were prominently identified as memory profiles at the epigenetic level. A similar pattern was previously found by Seaborne and colleagues *(Seaborne et al., 2018a)* in response to resistance training, demonstrating the presence of an epigenetic memory at DNA methylation level of previous training-induced hypertrophic stimulus, that led to the retention of hypomethylation during detraining, and subsequent larger hypomethylation after later retraining.

As reduced DNA methylation of genes generally leads to enhanced gene expression due to the removal of methylation, allowing improved access to the transcriptional

machinery and RNA polymerase that enable transcription, and also creating permissive euchromatin *(Rountree & Selker, 1997; Lunyak et al., 2002; Fuks et al., 2003; Bogdanović & Veenstra, 2009*). This would suggest that the earlier period of training leads to increased gene expression of this cluster of genes, which is then retained during detraining, to enable enhanced muscle adaptations, in the later retraining period. In the present study, deeply investigation of Signature 1 and 2, identified several regions located in or close to annotated genes with enriched differential methylation, that could likely be affected by more pronounced gene expression. Cross-reference with the most frequently occurring CpG modifications in pairwise comparisons of all conditions, resulted in identification of 11 genes following the temporal trend outlined by Signature 1 (Figure 17A) and Signature 2 (Figure 17B), that were examined gene expression by rt-qRT-PCR. Among these were found genes related to membrane proteins involved in cell-cell and cell-matrix interactions (*ADAM19*), membrane protein that mobilizes intracellular calcium (*INPP5a)*, synthesis of tetrahydrofolate in the mitochondrion (*MTHFD1L*), proteins of platelet-derived growth factors (PDGF) and vascular endothelial growth factors (VEGF) (*PDGFB*), calcium-activated neutral proteases calpains (*CAPN2*) and lactic acid and pyruvate transport across plasma membranes (*SLC16A3*). Importantly, these genes demonstrated a mirror/inverse relationship with DNA methylation of the CpG sites within the same genes (Figure 18). Where DNA methylation reduced after training, and was retained as hypomethylated into detraining and retraining, gene expression increased after training, and importantly, this increased expression was retained into detraining when exercise had completely ceased, and then subsequently retained as elevated into retraining. Overall, this suggested that these genes were hypomethylated and switched on after the earlier period of adaptations, maintained during cessation of exercise due to methylation of these genes remaining low, and retained as switched on or upregulated to even a greater extent upon exposure to a later period of high-intensity endurance retraining. This demonstrates that the methylation and collective responsiveness of these genes are important epigenetic regulators of skeletal muscle memory.

Results from the present study are in contrast with a previous transcriptomic study where authors, investigating gene expression via RNA sequencing in response to repeated unilateral endurance training, did not find evidence in support of the presence of a transcriptomic memory *(Lindholm et al., 2016)*. However, in the above study, DNA methylation was not investigated and more importantly, the exercise

paradigm involved was moderate-intensity endurance training, but as previously described, methylation and gene expression involved in metabolic and oxidative pathways are more affected with high-intensity exercise *(Barrès et al., 2012)*.

Among these six genes, INPP5a and CAPN2 are involved in calcium handling signaling, while SLC16A3 is involved in the lactate transport system. We decided to investigate these pathways through protein expression analysis. We identified that only the MCT1 protein (Figure 19A), which is crucial for the process of lactate transport into both sarcolemmal and mitochondrial membranes (*Dubouchaud et al., 2000*), exhibited a memory profile with a significant increase in expression after retraining. In contrast, proteins related to calcium pathways did not demonstrate any memory pattern in their expression profiles throughout the observed period. This discrepancy may be attributed to the complexity of the signaling pathway involved in calcium handling, where numerous genes impact the process. In contrast, the lactate transport system is regulated by a smaller set of genes, among which SLC16A3, which in the present study displayed a memory pattern in terms of epigenetic and transcriptional regulation, leading to a more evident memory effect at the functional level in the lactate metabolism.

## CONCLUSIVE REMARKS

High-intensity interval training resulted in an improvement in aerobic fitness, as indicated by the enhancement of functional indexes of endurance performance collected at the whole-body level. The increase in skeletal muscle capillary density paralleled changes in *in vivo* functional indexes, indicating that vascular changes in peripheral muscle work in conjunction with central changes to contribute to the gain of endurance performance with high-intensity interval training. Exposure to repeated high-intensity interval training interventions separated by a period of detraining resulted in similar adaptations of the same magnitude for both endurance performance and capillarization.

The mitochondrial adaptations identified in response to high-intensity interval training suggest an increase in mitochondrial biogenesis and content, as well as a mitochondrial pro-fusion effect. These findings are consistent with the expected outcomes of aerobic exercise training. However, there was no evidence of an effect on mitochondrial respiration.

The adaptations of mitochondria to high-intensity interval training differ depending on whether the stimulus has been previously encountered. Protein expression levels of markers for mitochondrial content, biogenesis, dynamics, and the endothelial marker CD31 tended to increase after the first training, were maintained during detraining and were further enhanced after retraining. The observed protein adaptation profile was not due to a transition in fibre types. Furthermore, the cross-sectional area of individual muscle fibres remained constant throughout the interventions, speculating that myonuclei incorporation did not significantly contribute to the observed increase in protein content.

Based on these observations, it is reasonable to hypothesize that some molecular adaptations to repeated high-intensity interval training interventions may be modulated by an epigenetically based memory mechanism.

Consistent with this hypothesis, epigenetic analyses revealed two memory profiles characterized by a state of hypomethylation that is acquired during training and maintained during detraining (with slight differences between the two signatures) and retraining. Some gene clusters delineated by both signatures exhibited a cumulative increase in gene expression during training and retention during detraining and retraining.

The temporal gene expression pattern of these genes showed an inverse relationship between methylation and gene expression. Specifically, after 8 weeks of high-intensity interval training, hypomethylation of these genes was associated with increased gene expression. This hypomethylation persisted during detraining, even when exercise training was completely interrupted, and gene expression remained elevated.

The genes responsible for maintaining transcript expression were primarily those associated with lactate transport and calcium signaling. Only the MCT1, which is involved in lactate transport, exhibited a protein memory profile. Proteins related to calcium pathways did not demonstrate any memory pattern in their expression profiles throughout the observed period.

The difference in the number of genes regulating the calcium handling and lactate transport systems may explain the observed discrepancy. The calcium handling pathway involves numerous genes, while the lactate transport system is regulated by a smaller set of genes. One of these genes, SLC16A3, exhibits a memory pattern in terms of epigenetic and transcriptional regulation, resulting in a more pronounced memory effect at the protein level in lactate metabolism.

It is important to consider that other factors, such as transcriptional regulation, post-transcriptional modifications, or protein degradation processes, may independently modulate protein levels, regardless of changes in DNA methylation. Additionally, the high degree of inter-individual variability, particularly in protein levels, may have hindered the identification of a protein profile that reflects epigenetic and gene expression. Furthermore, the study did not investigate the mtDNA methylome, which plays a crucial role in mitochondrial function and oxidative metabolism. This may explain why no mitochondrial pathways were found to be affected by epigenetic changes.

In conclusion, the present study provides evidence for an epigenetic muscle memory mechanism elicited by repeated high-intensity endurance training.

# References


**A**ndersen P, Henriksson J. Training induced changes in the subgroups of human type II skeletal muscle fibres. Acta Physiol Scand. 1977 Jan;99(1):123-5. doi: 10.1111/j.1748-1716.1977.tb10361.x. PMID: 842360.

**B**arrès R, Yan J, Egan B, Treebak JT, Rasmussen M, Fritz T, Caidahl K, Krook A, O'Gorman DJ & Zierath JR (2012). Acute exercise remodels promoter methylation in human skeletal muscle. Cell Metab 15, 405–411.

**B**atterson PM, McGowan EM, Stierwalt HD, Ehrlicher SE, Newsom SA, Robinson MM. Two weeks of high-intensity interval training increases skeletal muscle mitochondrial respiration via complex-specific remodeling in sedentary humans. J Appl Physiol (1985). 2023 Feb 1;134(2):339-355. doi: 10.1152/japplphysiol.00467.2022. Epub 2023 Jan 5. PMID: 36603044.

**B**azgir B, Fathi R, Rezazadeh Valojerdi M, Mozdziak P, Asgari A. Satellite Cells Contribution to Exercise Mediated Muscle Hypertrophy and Repair. Cell J. 2017 Winter;18(4):473-484. doi: 10.22074/cellj.2016.4714. Epub 2016 Sep 26. PMID: 28042532; PMCID: PMC5086326.

**B**eaver WL, Wasserman K & Whipp BJ (1986). A new method for detecting anaerobic threshold by gas exchange. J Appl Physiol 60, 2020–2027.

**B**ishop DJ, Granata C, Eynon N. 2014. Can we optimise the exercise training prescription to maximise improvements in mitochondria function and content? *Biochim Biophys Acta* 1840: 1266–1275.

**B**odine SC. mTOR signaling and the molecular adaptation to resistance exercise. Med Sci Sports Exerc. 2006 Nov;38(11):1950-7. doi: 10.1249/01.mss.0000233797.24035.35. PMID: 17095929

**B**ogdanović O & Veenstra GJC (2009). DNA methylation and methyl-CpG binding proteins: developmental requirements and function. Chromosoma 118, 549–565.

**B**ooth F.W., Ruegsegger G.N., Toedebusch R.G., Yan Z. Endurance Exercise and the Regulation of Skeletal Muscle Metabolism. Prog. Mol. Biol. Transl. Sci. 2015; 135:129–151. doi: 10.1016/bs.pmbts.2015.07.016.

**B**ooth FW, Thomason DB. Molecular and cellular adaptation of muscle in response to exercise: perspectives of various models. Physiol Rev. 1991 Apr;71(2):541-85. doi: 10.1152/physrev.1991.71.2.541. PMID: 2006222.

**B**rocca L, McPhee JS, Longa E, Canepari M, Seynnes O, De Vito G, Pellegrino MA, Narici M & Bottinelli R (2017). Structure and function of human muscle fibres and muscle proteome in physically active older men. J Physiol 595, 4823.

**B**ruusgaard JC, Gundersen K. In vivo time-lapse microscopy reveals no loss of murine myonuclei during weeks of muscle atrophy. J Clin Invest. 2008 Apr;118(4):1450-7. doi: 10.1172/JCI34022. PMID: 18317591; PMCID: PMC2262032.

**B**ruusgaard JC, Johansen IB, Egner IM, Rana ZA, Gundersen K (2010) Myonuclei acquired by overload exercise precede hypertrophy and are not lost on detraining. Proc Natl Acad Sci USA 107:15111–15116.

**B**urgomaster KA, Howarth KR, Phillips SM, Rakobowchuk M, Macdonald MJ, Mcgee SL & Gibala MJ (2008). Similar metabolic adaptations during exercise after low volume sprint interval and traditional endurance training in humans. *J Physiol* **586,** 151–160.

**C**aligiuri G. Mechanotransduction, immunoregulation, and metabolic functions of CD31 in cardiovascular pathophysiology. Cardiovasc Res. 2019 Jul 1;115(9):1425-1434. doi: 10.1093/cvr/cvz132. PMID: 31119265.

**C**amera DM, Smiles WJ, Hawley JA. Exercise-induced skeletal muscle signaling pathways and human athletic performance. Free Radic Biol Med. 2016 Sep;98:131-143. doi: 10.1016/j.freeradbiomed.2016.02.007. Epub 2016 Feb 11. PMID: 26876650.

**C**annavino J, Brocca L, Sandri M, Bottinelli R & Pellegrino MA (2014). PGC1-α over-expression prevents metabolic alterations and soleus muscle atrophy in hindlimb unloaded mice. J Physiol 592, 4575–4589.

**C**arson JA, Nettleton D, Reecy JM. Differential gene expression in the rat soleus muscle during early work overload-induced hypertrophy. FASEB J. 2002 Feb;16(2):207-9. doi: 10.1096/fj.01-0544fje. Epub 2001 Dec 14. PMID: 11744623.

**C**artoni, R. et al. Mitofusins 1/2 and ERRalpha expression are increased in human skeletal muscle after physical exercise. J. Physiol. 567, 349–358 (2005).

**C**han DC. Mitochondrial Dynamics and Its Involvement in Disease. Annu Rev Pathol. 2020 Jan 24;15:235-259. doi: 10.1146/annurev-pathmechdis-012419-032711. Epub 2019 Oct 4. PMID: 31585519.

**C**offey VG, Hawley JA. The molecular bases of training adaptation. Sports Med. 2007;37(9):737-63. doi: 10.2165/00007256-200737090-00001. PMID: 17722947.

**D**el Giudice M, Bonafiglia JT, Islam H, Preobrazenski N, Amato A & Gurd BJ (2020). Investigating the reproducibility of maximal oxygen uptake responses to high-intensity interval training. J Sci Med Sport 23, 94–99.

**D**u P, Zhang X, Huang CC, Jafari N, Kibbe WA, Hou L & Lin SM (2010). Comparison of Beta-value and M-value methods for quantifying methylation levels by microarray analysis. *BMC Bioinformatics*; DOI: 10.1186/1471-2105-11-587.

**D**ubouchaud H, Butterfield GE, Wolfel EE, Bergman BC, Brooks GA. Endurance training, expression, and physiology of LDH, MCT1, and MCT4 in human skeletal muscle. Am J Physiol Endocrinol Metab. 2000 Apr;278(4):E571-9. doi: 10.1152/ajpendo.2000.278.4.E571. PMID: 10751188.

**E**gan B & Zierath JR (2013). Exercise metabolism and the molecular regulation of skeletal muscle adaptation. Cell Metab 17, 162–184.

**E**gner IM, Bruusgaard JC, Eftestøl E & Gundersen K (2013). A cellular memory mechanism aids overload hypertrophy in muscle long after an episodic exposure to anabolic steroids. *J Physiol* **591,** 6221–6230.

**F**ernandez-Marcos P.J., Auwerx J. Regulation of PGC-1α, a nodal regulator of mitochondrial biogenesis. Am. J. Clin. Nutr. 2011; 93:884S–890S. doi:10.3945/ajcn.110.001917.

**F**errara N. Molecular and biological properties of vascular endothelial growth factor. J Mol Med (Berl). 1999 Jul;77(7):527-43. doi: 10.1007/s001099900019. PMID: 10494799.

**F**erraro E, Giammarioli AM, Chiandotto S, Spoletini I, Rosano G. Exercise-induced skeletal muscle remodeling and metabolic adaptation: redox signaling and role of autophagy. Antioxid Redox Signal. 2014 Jul 1;21(1):154-76. doi: 10.1089/ars.2013.5773. Epub 2014 Mar 6. PMID: 24450966; PMCID: PMC4048572.

**F**lück M, Hoppeler H. Molecular basis of skeletal muscle plasticity--from gene to form and function. Rev Physiol Biochem Pharmacol. 2003;146:159-216. doi: 10.1007/s10254-002-0004-7. Epub 2003 Jan 14. PMID: 12605307.

**F**rosig C, Jorgensen SB, Hardie DG, Richter EA, Wojtaszewski JF. 5′-AMP-activated protein kinase activity and protein expression are regulated by endurance training in human skeletal muscle. Am J Physiol. 2004;286:E411-7.

**F**uks F, Hurd PJ, Wolf D, Nan X, Bird AP & Kouzarides T (2003). The methyl-CpG-binding protein MeCP2 links DNA methylation to histone methylation. J Biol Chem 278, 4035–4040.

**G**arnier A, Fortin D, Zoll J, N'Guessan B, Mettauer B, Lampert E, Veksler V, Ventura-Clapier R. Coordinated changes in mitochondrial function and biogenesis in healthy and diseased human skeletal muscle. FASEB J. 2005 Jan;19(1):43-52. doi: 10.1096/fj.04-2173com. PMID: 15629894.

**G**eng, T., Li, P., Okutsu, M., Yin, X., Kwek, J., Zhang, M., & Yan, Z. (2010). PGC-1α plays a functional role in exercise-induced mitochondrial biogenesis and angiogenesis but not fiber-type transformation in mouse skeletal muscle. American Journal of Physiology-Cell Physiology, 298(3), C572-C579.

**G**ibala MJ, Little JP, van Essen M, Wilkin GP, Burgomaster KA, Safdar A, Raha S & Tarnopolsky MA (2006). Short-term sprint interval versus traditional endurance training: Similar initial adaptations in human skeletal muscle and exercise performance. *J Physiol* **575,** 901–911.

**G**liemann L, Gunnarsson TP, Hellsten Y, Bangsbo J. 10-20-30 training increases performance and lowers blood pressure and VEGF in runners. Scand J Med Sci Sports. 2015 Oct;25(5):e479-89. doi: 10.1111/sms.12356. Epub 2014 Dec 1. PMID: 25439558.

**G**oh Q, Song T, Petrany MJ, Cramer AA, Sun C, Sadayappan S, Lee SJ, Millay DP. Myonuclear accretion is a determinant of exercise-induced remodeling in skeletal muscle. Elife. 2019 Apr 23;8:e44876. doi: 10.7554/eLife.44876. PMID: 31012848; PMCID: PMC6497442.

**G**ranata C, Jamnick NA & Bishop DJ (2018). Training-Induced Changes in Mitochondrial Content and Respiratory Function in Human Skeletal Muscle. Sport Med 48, 1809–1828.

**G**ranata C, Oliveira RS, Little JP, Renner K, Bishop DJ. 2016a. Mitochondrial adaptations to high-volume exercise training are rapidly reversed after a reduction in training volume in human skeletal muscle. *FASEB J* 30: 3413–3423.

**G**undersen K. Excitation-transcription coupling in skeletal muscle: the molecular pathways of exercise. Biol Rev Camb Philos Soc. 2011 Aug;86(3):564-600. doi: 10.1111/j.1469-185X.2010.00161.x. Epub 2010 Oct 6. PMID: 21040371; PMCID: PMC3170710.

**G**ute D, Fraga C, Laughlin MH, Amann JF. Regional changes in capillary supply in skeletal muscle of high-intensity endurance-trained rats. J Appl Physiol (1985). 1996 Aug;81(2):619-26. doi: 10.1152/jappl.1996.81.2.619. PMID: 8872626.

**H**ellsten Y, Nyberg M. Cardiovascular Adaptations to Exercise Training. Compr Physiol. 2015 Dec 15;6(1):1-32. doi: 10.1002/cphy.c140080. PMID: 26756625.

**H**oier B, Passos M, Bangsbo J, Hellsten Y. Intense intermittent exercise provides weak stimulus for vascular endothelial growth factor secretion and capillary growth in skeletal muscle. Exp Physiol. 2013 Feb;98(2):585-97. doi: 10.1113/expphysiol.2012.067967. Epub 2012 Sep 7. PMID: 22962287.

**H**oier B, Prats C, Qvortrup K, Pilegaard H, Bangsbo J, Hellsten Y. Subcellular localization and mechanism of secretion of vascular endothelial growth factor in human skeletal muscle. FASEB J. 2013b Sep;27(9):3496-504. doi: 10.1096/fj.12-224618. Epub 2013 May 24. PMID: 23709615.

**H**ostrup M, Lemminger AK, Stocks B, Gonzalez-Franquesa A, Larsen JK, Quesada JP, Thomassen M, Weinert BT, Bangsbo J, Deshmukh AS. High-intensity interval training remodels the proteome and acetylome of human skeletal muscle. Elife. 2022 May 31;11:e69802. doi: 10.7554/eLife.69802. PMID: 35638262; PMCID: PMC9154743.

**H**uertas, J. R., Ruiz-Ojeda, F. J., Plaza-Díaz, J., Nordsborg, N. B., Martín-Albo, J., Rueda-Robles, A., & Casuso, R. A. (2019). Human muscular mitochondrial fusion in athletes during exercise. *The FASEB Journal*, *33*(11), 12087-12098.

**H**ughes DC, Ellefsen S, Baar K. Adaptations to Endurance and Strength Training. Cold Spring Harb Perspect Med. 2018 Jun 1;8(6):a029769. doi: 10.1101/cshperspect.a029769. PMID: 28490537; PMCID: PMC5983157.

**I**shihara N, Eura Y, Mihara K. Mitofusin 1 and 2 play distinct roles in mitochondrial fusion reactions via GTPase activity. J Cell Sci. 2004 Dec 15;117(Pt 26):6535-46. doi: 10.1242/jcs.01565. Epub 2004 Nov 30. PMID: 15572413.

**J**acques M, Hiam D, Craig J, Barrès R, Eynon N, Voisin S. Epigenetic changes in healthy human skeletal muscle following exercise- a systematic review. Epigenetics. 2019 Jul;14(7):633-648. doi: 10.1080/15592294.2019.1614416. Epub 2019 May 13. PMID: 31046576; PMCID: PMC6557592.

**J**ensen L, Bangsbo J, Hellsten Y. Effect of high intensity training on capillarization and presence of angiogenic factors in human skeletal muscle. J Physiol. 2004 Jun 1;557(Pt 2):571-82. doi: 10.1113/jphysiol.2003.057711. Epub 2004 Mar 12. PMID: 15020701; PMCID: PMC1665084.

**J**oanisse S, McKay BR, Nederveen JP, Scribbans TD, Gurd BJ, Gillen JB, et al. Satellite cell activity, without expansion, after nonhypertrophic stimuli. Am J Physiol Regul Integr Comp Physiol. 2015;309(9):R1101–11.

**K**anehisa M & Goto S (2000). KEGG: kyoto encyclopedia of genes and genomes. Nucleic Acids Res 28, 27–30.

**K**anehisa M, Furumichi M, Tanabe M, Sato Y & Morishima K (2017). KEGG: new perspectives on genomes, pathways, diseases and drugs. Nucleic Acids Res 45, D353–D361.

**K**anehisa M, Sato Y, Kawashima M, Furumichi M & Tanabe M (2016). KEGG as a reference resource for gene and protein annotation. Nucleic Acids Res 44, D457–D462.

**K**anzleiter T, Jähnert M, Schulze G, Selbig J, Hallahan N, Schwenk RW, Schürmann A. Exercise training alters DNA methylation patterns in genes related to muscle growth and differentiation in mice. Am J Physiol Endocrinol Metab. 2015 May 15;308(10):E912-20. doi: 10.1152/ajpendo.00289.2014. Epub 2015 Mar 24. PMID: 25805191.

**K**ohn TA, Essén-Gustavsson B, Myburgh KH. Specific muscle adaptations in type II fibers after high-intensity interval training of well-trained runners. Scand J Med Sci Sports. 2011 Dec;21(6):765-72. doi: 10.1111/j.1600-0838.2010.01136.x. Epub 2010 May 12. PMID: 20492589.

**K**oulmann N, Bigard AX. Interaction between signalling pathways involved in skeletal muscle responses to endurance exercise. Pflugers Arch. 2006 May;452(2):125-39. doi: 10.1007/s00424-005-0030-9. Epub 2006 Jan 18. PMID: 16437222.

**L**aker RC, Lillard TS, Okutsu M, Zhang M, Hoehn KL, Connelly JJ, et al. Exercise prevents maternal high-fat diet-induced hypermethylation of the Pgc-1α gene and age-dependent metabolic dysfunction in the offspring. Diabetes. 2014;63:1605–11.

**L**antier, L., Fentz, J., Mounier, R., Leclerc, J., Treebak, J.T., Pehmøller, C., Sanz, N., Sakakibara, I., Saint-Amand, E., Rimbaud, S., Maire, P., Marette, A., Ventura-Clapier, R., Ferry, A., Wojtaszewski, J.F.P., Foretz, M. and Viollet, B. (2014), AMPK controls exercise endurance, mitochondrial oxidative capacity, and skeletal muscle integrity. The FASEB Journal, 28: 3211-3224. https://doi.org/10.1096/fj.14-250449

**L**arsen S, Nielsen J, Hansen CN, Nielsen LB, Wibrand F, Stride N, Schroder HD, Boushel R, Helge JW, Dela F, Hey-Mogensen M. Biomarkers of mitochondrial content in skeletal muscle of healthy young human subjects. J Physiol. 2012 Jul 15;590(14):3349-60. doi: 10.1113/jphysiol.2012.230185. Epub 2012 May 14. PMID: 22586215; PMCID: PMC3459047.

**L**ee H, Kim K, Kim B, Shin J, Rajan S, Wu J, Chen X, Brown MD, Lee S & Park JY (2018). A cellular mechanism of muscle memory facilitates mitochondrial remodelling following resistance training. *J Physiol* **596,** 4413–4426.

**L**i, J.; Li, Y.; Atakan, M.M.; Kuang, J.; Hu, Y.; Bishop, D.J.; Yan, X. The Molecular Adaptive Responses of Skeletal Muscle to High-Intensity Exercise/Training and Hypoxia. *Antioxidants* **2020**, *9*, 656. https://doi.org/10.3390/antiox9080656.

**L**indholm ME, Giacomello S, Werne Solnestam B, Fischer H, Huss M, Kjellqvist S & Sundberg CJ (2016). The Impact of Endurance Training on Human Skeletal Muscle Memory, Global Isoform Expression and Novel Transcripts. PLoS Genet; DOI: 10.1371/JOURNAL.PGEN.1006294.

**L**indholm ME, Marabita F, Gomez-Cabrero D, Rundqvist H, Ekström TJ, Tegnér J & Sundberg CJ (2014). An integrative analysis reveals coordinated reprogramming of the epigenome and the transcriptome in human skeletal muscle after training. *Epigenetics* **9,** 1557–1569.

**L**loyd EM, Pinniger GJ, Murphy RM, Grounds MD. Slow or fast: Implications of myofibre type and associated differences for manifestation of neuromuscular disorders. Acta Physiol (Oxf). 2023 Aug;238(4):e14012. doi: 10.1111/apha.14012. Epub 2023 Jul 21. PMID: 37306196.

**L**ochmann TL, Thomas RR, Bennett JP Jr, Taylor SM. Epigenetic modifications of the PGC-1α promoter during exercise induced expression in mice. PLoS One. 2015;10(6):e0129647.

**L**unyak V V., Burgess R, Prefontaine GG, Nelson C, Sze SH, Chenoweth J, Schwartz P, Pevzner PA, Glass C, Mandel G & Rosenfeld MG (2002). Corepressor-dependent silencing of chromosomal regions encoding neuronal genes. Science 298, 1747–1752.

**M**aasar MF, Turner DC, Gorski PP, Seaborne RA, Strauss JA, Shepherd SO, Cocks M, Pillon NJ, Zierath JR, Hulton AT, Drust B, Sharples AP. The Comparative Methylome and Transcriptome After Change of Direction Compared to Straight Line Running Exercise in Human Skeletal Muscle. Front Physiol. 2021 Feb 19;12:619447. doi: 10.3389/fphys.2021.619447. PMID: 33679435; PMCID: PMC7933519.

**M**aksimovic J, Phipson B & Oshlack A (2017). A cross-package Bioconductor workflow for analysing methylation array data. F1000Research; DOI: 10.12688/F1000RESEARCH.8839.3/DOI.

Maksimovic J, Phipson B & Oshlack A (2017). A cross-package Bioconductor workflow for analysing methylation array data. *F1000Research*; DOI: 10.12688/F1000RESEARCH.8839.3/DOI.

**M**alek MH, Olfert IM, Esposito F. Detraining losses of skeletal muscle capillarization are associated with vascular endothelial growth factor protein expression in rats. Exp Physiol. 2010 Feb;95(2):359-68. doi: 10.1113/expphysiol.2009.050369. Epub 2009 Oct 30. PMID: 19880536.

**M**arcangeli, V., Youssef, L., Dulac, M., Carvalho, L. P., Hajj-Boutros, G., Reynaud, O.,& Gouspillou, G. (2022). Impact of high-intensity interval training with or without l-citrulline on physical performance, skeletal muscle, and adipose tissue in obese older adults. *Journal of Cachexia, Sarcopenia and Muscle*, *13*(3), 1526-1540.

**M**cConell GK, Lee-Young RS, Chen ZP, Stepto NK, Huynh NN, Stephens TJ, Canny BJ, Kemp BE. Short-term exercise training in humans reduces AMPK signalling during prolonged exercise independent of muscle glycogen. J Physiol. 2005 Oct 15;568(Pt 2):665-76. doi: 10.1113/jphysiol.2005.089839. Epub 2005 Jul 28. PMID: 16051629; PMCID: PMC1474728.

**M**einild Lundby AK, Jacobs RA, Gehrig S, de Leur J, Hauser M, Bonne TC, Flück D, Dandanell S, Kirk N, Kaech A, Ziegler U, Larsen S, Lundby C. Exercise training increases skeletal muscle mitochondrial volume density by enlargement of existing mitochondria and not de novo biogenesis. Acta Physiol (Oxf). 2018 Jan;222(1). doi: 10.1111/apha.12905. Epub 2017 Jul 6. PMID: 28580772.

**M**ilkiewicz M, Brown MD, Egginton S, Hudlicka O. Association between shear stress, angiogenesis, and VEGF in skeletal muscles in vivo. Microcirculation. 2001 Aug;8(4):229-41. doi: 10.1038/sj/mn/7800074. PMID: 11528531.

**M**iyazaki M, Esser KA. Cellular mechanisms regulating protein synthesis and skeletal muscle hypertrophy in animals. J Appl Physiol (1985). 2009 Apr;106(4):1367-73. doi: 10.1152/japplphysiol.91355.2008. Epub 2008 Nov 26. PMID: 19036895; PMCID: PMC2698644.

**M**ontarras D, L'Honore A, Buckingham M (2013) Lying low but ready for action: the quiescent muscle satellite cell. FEBS J 280:4036–4050.

**M**ontero D, Cathomen A, Jacobs RA, Flück D, de Leur J, Keiser S, Bonne T, Kirk N, Lundby AK, Lundby C. Haematological rather than skeletal muscle adaptations contribute to the increase in peak oxygen uptake induced by moderate endurance training. J Physiol. 2015 Oct 15;593(20):4677-88. doi: 10.1113/JP270250. **E**pub 2015 Sep 14. Erratum in: J Physiol. 2018 Apr 1;596(7):1311. PMID: 26282186; PMCID: PMC4606528.

**M**urach KA, Dungan CM, Dupont-Versteegden EE, McCarthy JJ, Peterson CA. "Muscle memory" not mediated by myonuclear number? Secondary analysis of human detraining data. J Appl Physiol

(1985). 2019 Dec 1;127(6):1814-1816. doi: 10.1152/japplphysiol.00506.2019. Epub 2019 Sep 12. PMID: 31513448.

**N**ielsen J. N., Mustard K. J., Graham D. A., Yu H., MacDonald C. S., Pilegaard H., Goodyear L. J., Hardie D. G., Richter E. A., Wojtaszewski J. F. 5′-AMP-activated protein kinase activity and subunit expression in exercise-trained human skeletal muscle. J. Appl. Physiol. (1985). 94, 631–641.

**N**itert MD et al. (2012). Impact of an exercise intervention on DNA methylation in skeletal muscle from first-degree relatives of patients with type 2 diabetes. *Diabetes* **61,** 3322–3332.

**N**itert MD, Dayeh T, Volkov P, Elgzyri T, Hall E, Nilsson E, Yang BT, Lang S, Parikh H, Wessman Y, Weishaupt H, Attema J, Abels M, Wierup N, Almgren P, Jansson PA, Rönn T, Hansson O, Eriksson KF, Groop L, Ling C. Impact of an exercise intervention on DNA methylation in skeletal muscle from first-degree relatives of patients with type 2 diabetes. Diabetes. 2012 Dec;61(12):3322-32. doi: 10.2337/db11-1653. Epub 2012 Oct 1. PMID: 23028138; PMCID: PMC3501844.

**N**orrbom J, Sundberg CJ, Ameln H, Kraus WE, Jansson E, Gustafsson T. PGC-1alpha mRNA expression is influenced by metabolic perturbation in exercising human skeletal muscle. J Appl Physiol (1985). 2004 Jan;96(1):189-94. doi: 10.1152/japplphysiol.00765.2003. Epub 2003 Sep 12. PMID: 12972445.

**O'**Neil, T.K., L.R. Duffy, J.W. Frey, and T.A. Hornberger. 2009. The role of phosphoinositide 3-kinase and phosphatidic acid in the regulation of mammalian target of rapamycin following eccentric contractions. *J Physiol*. 587:3691-3701.

**P**erry CG, Kane DA, Lin CT, Kozy R, Cathey BL, Lark DS, Kane CL, Brophy PM, Gavin TP, Anderson EJ, Neufer PD. Inhibiting myosin-ATPase reveals a dynamic range of mitochondrial respiratory control in skeletal muscle. Biochem J. 2011 Jul 15;437(2):215-22. doi: 10.1042/BJ20110366. PMID: 21554250; PMCID: PMC3863643.

**P**esta D & Gnaiger E (2012). High-resolution respirometry: OXPHOS protocols for human cells and permeabilized fibers from small biopsies of human muscle. Methods Mol Biol 810, 25–58.

**P**hilp, A., D.L. Hamilton, and K. Baar. 2011. Signals mediating skeletal muscle remodeling by resistance exercise: PI3-kinase independent activation of mTORC1. *J Appl Physiol (1985)*. 110:561-568.

**P**idsley R, Zotenko E, Peters TJ, Lawrence MG, Risbridger GP, Molloy P, Van Djik S, Muhlhausler B, Stirzaker C & Clark SJ (2016). Critical evaluation of the Illumina MethylationEPIC BeadChip microarray for whole-genome DNA methylation profiling. Genome Biol; DOI: 10.1186/S13059-016-1066-1.

**P**rior BM, Yang HT, Terjung RL. What makes vessels grow with exercise training? J Appl Physiol (1985). 2004 Sep;97(3):1119-28. doi: 10.1152/japplphysiol.00035.2004. PMID: 15333630.

**P**silander N, Eftestøl E, Cumming KT, Juvkam I, Ekblom MM, Sunding K, Wernbom M, Holmberg HC, Ekblom B, Bruusgaard JC, Raastad T & Gundersen K (2019). Effects of training, detraining, and retraining on strength, hypertrophy, and myonuclear number in human skeletal muscle. *J Appl Physiol* **126,** 1636–1645.

**Q**aisar R, Bhaskaran S, Van Remmen H. Muscle fiber type diversification during exercise and regeneration. Free Radic Biol Med. 2016 Sep;98:56-67. doi: 10.1016/j.freeradbiomed.2016.03.025. Epub 2016 Mar 29. PMID: 27032709.

**R**obach P, Bonne T, Flück D, Bürgi S, Toigo M, Jacobs RA & Lundby C (2014). Hypoxic training: effect on mitochondrial function and aerobic performance in hypoxia. Med Sci Sports Exerc 46, 1936–1945.

**R**oss M, Kargl CK, Ferguson R, Gavin TP, Hellsten Y. Exercise-induced skeletal muscle angiogenesis: impact of age, sex, angiocrines and cellular mediators. Eur J Appl Physiol. 2023 Jul;123(7):1415-1432. doi: 10.1007/s00421-022-05128-6. Epub 2023 Jan 30. PMID: 36715739; PMCID: PMC10276083.

**R**ountree MR & Selker EU (1997). DNA methylation inhibits elongation but not initiation of transcription in Neurospora crassa. Genes Dev 11, 2383–2395.

**R**owlands DS, Page RA, Sukala WR, Giri M, Ghimbovschi SD, Hayat I, Cheema BS, Lys I, Leikis M, Sheard PW, Wakefield SJ, Breier B, Hathout Y, Brown K, Marathi R, Orkunoglu-Suer FE, Devaney JM, Leiken B, Many G, Krebs J, Hopkins WG, Hoffman EP. Multi-omic integrated networks connect DNA methylation and miRNA with skeletal muscle plasticity to chronic exercise in Type 2 diabetic obesity. Physiol Genomics. 2014 Oct 15;46(20):747-65. doi: 10.1152/physiolgenomics.00024.2014. Epub 2014 Aug 19. PMID: 25138607; PMCID: PMC4200377.

**R**uegsegger, Gregory N., et al. "High-intensity aerobic, but not resistance or combined, exercise training improves both cardiometabolic health and skeletal muscle mitochondrial dynamics." *Journal of Applied Physiology* 135.4 (2023): 763-774.

**S**andri M. Signaling in muscle atrophy and hypertrophy. Physiology (Bethesda). 2008 Jun;23:160-70. doi: 10.1152/physiol.00041.2007. PMID: 18556469.

**S**artori, R., Romanello, V. & Sandri, M. Mechanisms of muscle atrophy and hypertrophy: implications in health and disease. *Nat Commun* **12**, 330 (2021). https://doi.org/10.1038/s41467-020-20123-1

**S**carpulla RC. Transcriptional activators and coactivators in the nuclear control of mitochondrial function in mammalian cells. Gene. 2002 Mar 6;286(1):81-9. doi: 10.1016/s0378-1119(01)00809-5. PMID: 11943463.

**S**chiaffino S, Bormioli SP, Aloisi M (1972) Cell proliferation in rat skeletal muscle during early stages of compensatory hypertrophy. Virchows Archiv B Cell Pathol 11:268–273.

**S**chiaffino S, Bormioli SP, Aloisi M (1976) The fate of newly formed satellite cells during compensatory muscle hypertrophy. Virchows Archiv B Cell Pathol 21:113–118.

**S**chiaffino S, Reggiani C. Fiber types in mammalian skeletal muscles. Physiol Rev. 2011 Oct;91(4):1447-531. doi: 10.1152/physrev.00031.2010. PMID: 22013216.

**S**chiaffino S, Reggiani C. Molecular diversity of myofibrillar proteins: gene regulation and functional significance. Physiol Rev. 1996 Apr;76(2):371-423. doi: 10.1152/physrev.1996.76.2.371. PMID: 8618961.

**S**choenfeld BJ. The mechanisms of muscle hypertrophy and their application to resistance training. J Strength Cond Res. 2010 Oct;24(10):2857-72. doi: 10.1519/JSC.0b013e3181e840f3. PMID: 20847704.

**S**cribbans TD, Edgett BA, Vorobej K, Mitchell AS, Joanisse SD, Matusiak JB, Parise G, Quadrilatero J, Gurd BJ. Fibre-specific responses to endurance and low volume high intensity interval training: striking similarities in acute and chronic adaptation. PLoS One. 2014 Jun 5;9(6):e98119. doi: 10.1371/journal.pone.0098119. PMID: 24901767; PMCID: PMC4047011.

**S**eaborne RA, Strauss J, Cocks M, Shepherd S, O'brien TD, van Someren KA, Bell PG, Murgatroyd C, Morton JP, Stewart CE, Mein CA & Sharples AP (2018a). Methylome of human skeletal muscle after acute & chronic resistance exercise training, detraining & retraining. Sci Data; DOI: 10.1038/sdata.2018.213.

**S**eaborne RA, Strauss J, Cocks M, Shepherd S, O'Brien TD, Van Someren KA, Bell PG, Murgatroyd C, Morton JP, Stewart CE & Sharples AP (2018b). Human Skeletal Muscle Possesses an Epigenetic Memory of Hypertrophy. Sci Rep 8, 1–17.

**S**harples AP, Stewart CE & Seaborne RA (2016*b*). Does skeletal muscle have an 'epi'-memory? The role of epigenetics in nutritional programming, metabolic disease, aging and exercise. *Aging Cell* **15,** 603–616.

**S**imoneau JA, Lortie G, Boulay MR, Marcotte M, Thibault MC & Bouchard C (1987). Effects of two high-intensity intermittent training programs interspaced by detraining on human skeletal muscle and performance. Eur J Appl Physiol Occup Physiol 56, 516–521.

**S**mith JAB, Murach KA, Dyar KA, Zierath JR. Exercise metabolism and adaptation in skeletal muscle. Nat Rev Mol Cell Biol. 2023 Sep;24(9):607-632. doi: 10.1038/s41580-023-00606-x. Epub 2023 May 24. PMID: 37225892; PMCID: PMC10527431.

**S**nijders T, Leenders M, de Groot LCPGM, van Loon LJC, Verdijk LB. Muscle mass and strength gains following 6 months of resistance type exercise training are only partly preserved within one year with autonomous exercise continuation in older adults. Exp Gerontol. 2019 Jul 1;121:71-78. doi: 10.1016/j.exger.2019.04.002. Epub 2019 Apr 9. PMID: 30978433.

**S**olsona R, Pavlin L, Bernardi H, Sanchez AM. Molecular Regulation of Skeletal Muscle Growth and Organelle Biosynthesis: Practical Recommendations for Exercise Training. Int J Mol Sci. 2021 Mar 8;22(5):2741. doi: 10.3390/ijms22052741. PMID: 33800501; PMCID: PMC7962973.

**S**oriano FX, Liesa M, Bach D, Chan DC, Palacín M & Zorzano A (2006). Evidence for a mitochondrial regulatory pathway defined by peroxisome proliferator-activated receptor-gamma coactivator-1 alpha, estrogen-related receptor-alpha, and mitofusin 2. Diabetes 55, 1783–1791.

**S**tephens NA, Brouwers B, Eroshkin AM, Yi F, Cornnell HH, Meyer C, Goodpaster BH, Pratley RE, Smith SR & Sparks LM (2018). Exercise Response Variations in Skeletal Muscle PCr Recovery Rate and Insulin Sensitivity Relate to Muscle Epigenomic Profiles in Individuals With Type 2 Diabetes. Diabetes Care 41, 2245–2254.

**T**an R, Nederveen JP, Gillen JB, Joanisse S, Parise G, Tarnopolsky MA, Gibala MJ. Skeletal muscle fiber-type-specific changes in markers of capillary and mitochondrial content after low-volume interval training in overweight women. Physiol Rep. 2018 Mar;6(5):e13597. doi: 10.14814/phy2.13597. PMID: 29484852; PMCID: PMC5827496.

**T**ezze, C., Romanello, V., Desbats, M. A., Fadini, G. P., Albiero, M., Favaro, G., ... & Sandri, M. (2017). Age-associated loss of OPA1 in muscle impacts muscle mass, metabolic homeostasis, systemic inflammation, and epithelial senescence. *Cell metabolism*, *25*(6), 1374-1389.

**T**jønna AE, Lee SJ, Rognmo Ø, Stølen TO, Bye A, Haram PM, Loennechen JP, Al-Share QY, Skogvoll E, Slørdahl SA, Kemi OJ, Najjar SM, Wisløff U. Aerobic interval training versus continuous moderate exercise as a treatment for the metabolic syndrome: a pilot study. Circulation. 2008 Jul 22;118(4):346-54. doi: 10.1161/CIRCULATIONAHA.108.772822. Epub 2008 Jul 7. PMID: 18606913; PMCID: PMC2777731.

**T**urner DC, Seaborne RA, Sharples AP. Comparative Transcriptome and Methylome Analysis in Human Skeletal Muscle Anabolism, Hypertrophy and Epigenetic Memory. Sci Rep. 2019 Mar 12;9(1):4251. doi: 10.1038/s41598-019-40787-0. PMID: 30862794; PMCID: PMC6414679.

**V**ierck J, O'Reilly B, Hossner K, Antonio J, Byrne K, Bucci L, Dodson M. Satellite cell regulation following myotrauma caused by resistance exercise. Cell Biol Int. 2000;24(5):263-72. doi: 10.1006/cbir.2000.0499. PMID: 10805959.

**W**hipp BJ, Davis JA, Torres F & Wasserman K (1981). A test to determine parameters of aerobic function during exercise. J Appl Physiol 50, 217–221.

**W**isløff U, Støylen A, Loennechen JP, Bruvold M, Rognmo Ø, Haram PM, Tjønna AE, Helgerud J, Slørdahl SA, Lee SJ, Videm V, Bye A, Smith GL, Najjar SM, Ellingsen Ø, Skjaerpe T. Superior cardiovascular effect of aerobic interval training versus moderate continuous training in heart failure patients: a randomized study. Circulation. 2007 Jun 19;115(24):3086-94. doi: 10.1161/CIRCULATIONAHA.106.675041. Epub 2007 Jun 4. PMID: 17548726.

**W**ittwer M, Flück M, Hoppeler H, Muller S, Desplanches D, Billeter R (2002) Prolonged unloading of rat soleus muscle causes distinct adaptations of the gene profile. FASEB J 16:884-886.

**Y**amada, A.K., R. Verlengia, and C.R. Bueno Junior. 2012. Mechanotransduction pathways in skeletal muscle hypertrophy. *J Recept Signal Transduct Res*. 32:42-44.

**Y**oule RJ, van der Bliek AM. Mitochondrial fission, fusion, and stress. Science. 2012 Aug 31;337(6098):1062-5. doi: 10.1126/science.1219855. PMID: 22936770; PMCID: PMC4762028.

**Z**hang L, Zhou Y, Wu W, Hou L, Chen H, Zuo B, Xiong Y, Yang J. Skeletal Muscle-Specific Overexpression of PGC-1α Induces Fiber-Type Conversion through Enhanced Mitochondrial Respiration and Fatty Acid Oxidation in Mice and Pigs. Int J Biol Sci. 2017 Sep 5;13(9):1152-1162. doi: 10.7150/ijbs.20132. PMID: 29104506; PMCID: PMC5666330.

**Z**uccarelli L, Baldassarre G, Magnesa B, Degano C, Comelli M, Gasparini M, Manferdelli G, Marzorati M, Mavelli I, Pilotto A, Porcelli S, Rasica L, Šimunič B, Pišot R, Narici M & Grassi B (2021). Peripheral impairments of oxidative metabolism after a 10-day bed rest are upstream of mitochondrial respiration. J Physiol 599, 4813–4829.